CHEMISTRY
A EUROPEAN JOURNAL

DOI: 10.1002/chem.201102145

Rare-Earth Metal Allyl and Hydrido Complexes Supported by an (NNNN)-Type Macrocyclic Ligand: Synthesis, Structure, and Reactivity toward Biomass-Derived Furanics

Elise Abinet, Daniel Martin, Sabine Standfuss, Heiko Kulinna, Thomas P. Spaniol, and Jun Okuda*[a]

Abstract: The preparation and characterization of a series of neutral rare-earth metal complexes [Ln(Me_3TACD)(η^3-C_3H_5)$_2$] (Ln = Y, La, Ce, Pr, Nd, Sm) supported by the 1,4,7-trimethyl-1,4,7,10-tetraazacyclododecane anion (Me_3TACD$^-$) are reported. Upon treatment of the neutral allyl complexes [Ln(Me_3TACD)(η^3-C_3H_5)$_2$] with Brønsted acids, monocationic allyl complexes [Ln(Me_3TACD)(η^3-C_3H_5)(thf)$_2$][B(C_6X_5)$_4$] (Ln = La, Ce, Nd, X = H, F) were isolated and characterized. Hydrogenolysis gave the hydride complexes [Ln(Me_3TACD)H_2]$_n$ (Ln = Y, n = 3; La, n = 4; Sm). X-ray crystallography showed the lanthanum hydride to be tetranuclear. Reactivity studies of [Ln(Me_3TACD)R_2]$_n$ (R = η^3-C_3H_5, n = 0; R = H, n = 3,4) towards furan derivatives includes hydrosilylation and deoxygenation under ring-opening conditions.

Keywords: allyl ligands · hydrodeoxygenation · hydrosilylation · lanthanides · macrocyclic ligands

Introduction

Lignocellulosic biomass from wood or paper waste is a renewable carbon-neutral source of energy, which does not compete with food production such as corn or sugar cane and could reduce society's dependence on petroleum.[1] Lignocellulosic biomass is separated into its three main constituents: 40–80% cellulose, 15–30% hemicellulose, and 10–25% lignin.[1b] Subsequent acid treatment of hemicellulose leads to pentoses, which can be transformed into furfural with sulfuric acid.[2] Dehydration of glucose from cellulose gives 5-hydroxymethylfurfural (HMF),[3] but furfural and its derivatives are not suitable as fuels for combustion engines. Hence, further transformations are needed to obtain the next generation of biofuels.[1,4] Highly Lewis acidic rare-earth metal complexes hold promise as new catalysts for the conversion of furanics. We describe here the synthesis and characterization of rare-earth metal complexes supported by Me_3TACD$^-$ ((Me_3TACD)H = Me_3[12]aneN4:1,4,7-trimethyl-1,4,7,10-tetraazacyclododecane) along with their reactivity for the conversion of furanics. Me_3TACD$^-$ is a monoanionic (NNNN)-type ligand,[5] introduced in 1985 by Lehn et al. as an appropriate complexation agent for divalent copper and later for other metals.[6a,7a,b,8] As a ten-electron donor, Me_3TACD$^-$ coordinates facially at trivalent rare-earth metals and shields one hemisphere of the large metal center.[7a,b] Alkyl and hydrido complexes of the smaller rare-earth metals [Ln(Me_3TACD)R_2]$_n$ (Ln = Sc, Y, Ho, Lu, R = CH_2SiMe_3, n = 1 or Ln = Y, Ho, Lu, R = H, n = 3) catalyze the hydrosilylation of α-olefins.[7a,b] Heavy lanthanides are rare and expensive for technical applications, whereas the natural abundance of the lighter lanthanides, especially of the most abundant rare-earth metal cerium,[9] has motivated us to use these metals. A further modification is the replacement of the thermally labile trimethylsilylmethyl ligand by allyl ligands η^3-C_3H_5 that can stabilize large rare-earth metals.[10]

Results and Discussion

Ligand synthesis: All reported synthetic pathways to the proligand (Me_3TACD)H (**L**H) are tedious and low-yielding procedures.[6] We have now developed a two-step synthesis with an overall yield of 72% starting from commercially available cyclen (Scheme 1). In the first step, 1,4,7-triformylcyclen was prepared from cyclen by using three equivalents

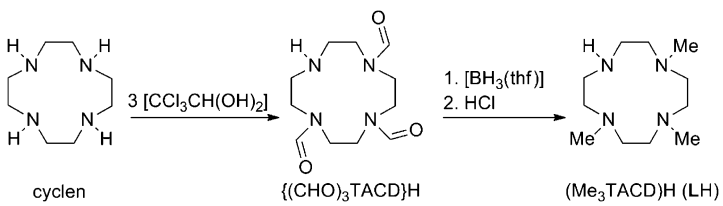

Scheme 1. Improved synthesis of (Me_3TACD)H (**L**H).

[a] Dipl.-Chem. E. Abinet, Dipl.-Chem. D. Martin, Dipl.-Chem. S. Standfuss, Dipl.-Chem. H. Kulinna, Dr. T. P. Spaniol, Prof. Dr. J. Okuda
Institut für Anorganische Chemie
RWTH Aachen University
Landoltweg 1, 52056 Aachen (Germany)
Fax: (+49) 241-80-92644
E-mail: jun.okuda@ac.rwth-aachen.de

of chloral hydrate.[11] Reduction of the formyl groups to methyl groups with $[BH_3(thf)]$,[12] followed by treatment with hydrochloric acid and subsequent workup led to **L**H.

The monohydrochloride **L**H·HCl was extracted from aqueous solution at pH 13 by using dichloromethane and recrystallized to give X-ray quality crystals.[5c] The solid structure reveals a C_s-symmetric ring (Figure 1). The hole size

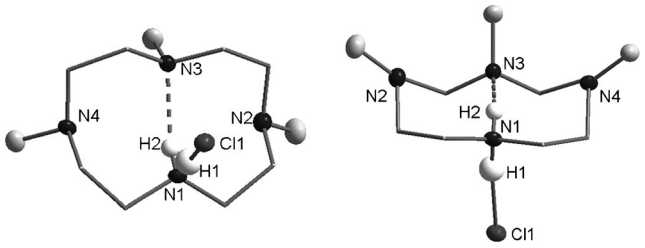

Figure 1. Molecular structure of $[(Me_3TACD)H_2]^+Cl^-$ (**L**H·HCl). Thermal ellipsoids are drawn at the 50% probability level. Hydrogen atoms in the ethylene bridge are omitted for clarity.

r(H) is commonly used to compare the size of the cavity within a macrocyclic ligand.[13] The radius of the available cavity[13a] in **L**H·HCl (r(H) = 1.244(2) Å) is smaller than in the hydrochloride of cyclen (r(H) = 1.9 Å).[13b–f] The hole size in $[(cyclen)H]^+Cl^-$ is larger than in **L**H·HCl, but a closer look reveals different conformations adopted in their solid structures (Figure 2). In cyclen, the nitrogen atoms

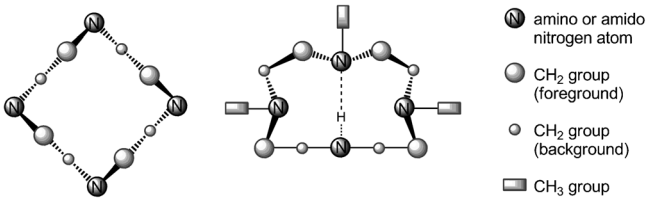

Figure 2. Schematic conformation modes of the hydrochloric salt of cyclen (left) and $[(Me_3TACD)H_2]^+Cl^-$ (**L**H·HCl, right).

point away from the ring system in an exocyclic mode, whereas in $[(Me_3TACD)H_2]^+Cl^-$ the nitrogen atoms bind in endocyclic fashion, forming a rectangle caused by an intra-annular hydrogen bridge between H2 and N3.[13e] The hydrogen bonding found between protonated N1 and N3 reveals an interatomic distance of 2.814(4) Å, which is shorter than in the analogous mono(hydrochloride) salt of 1,4,7-tris(*tert*-butoxycarbonylmethyl)-1,4,7,10-tetraazacyclododecane.[14]

Neutral bis(allyl) complexes: The solvent-free bis(allyl) complexes $[Ln(Me_3TACD)(\eta^3\text{-}C_3H_5)_2]$ (Ln = Y **1-Y**, La **1-La**, Ce **1-Ce**, Pr **1-Pr**, Nd **1-Nd**, Sm **1-Sm**) were synthesized from the thermally stable tris(allyl) complexes $[Ln(\eta^3\text{-}C_3H_5)_3(1,4\text{-dioxane})]$[15] (Scheme 2). X-ray diffraction quality crystals of the complexes **1-Y**, **1-La**, **1-Pr**, and **1-Sm** were grown at −40 °C (Figure 3, Table 1). The geometry around the metal

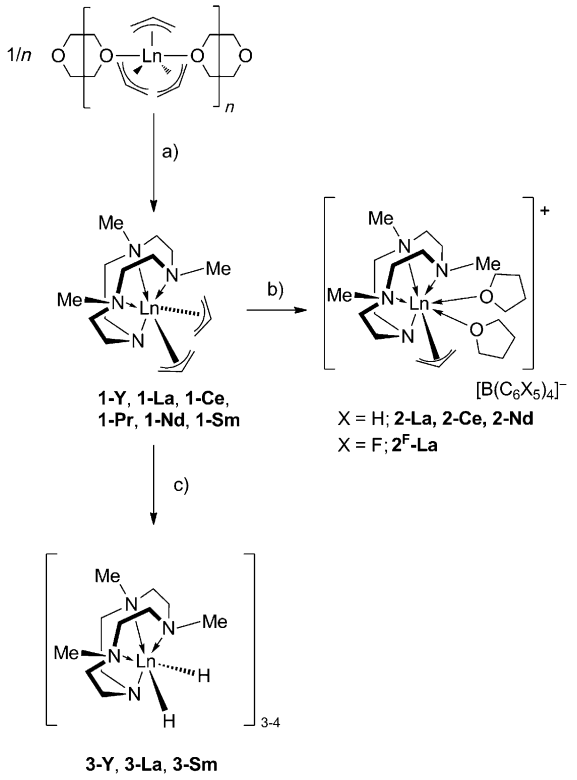

Scheme 2. General synthetic routes: a) **L**H, THF, 3 h, RT; b) $[NEt_3H][B(C_6X_5)_4]$ (X = H, F), THF, 1.5 h, RT; c) THF, $p(H_2)$ = 5 bar, 3 days, 50 °C or $PhSiH_3$ (1.5 equiv), RT, 1 h.

centers is similar and is best described as a square antiprism formed by the nitrogen atoms of the ligand and the terminal carbon atoms of both allyl ligands. Compounds **1-Pr** and **1-Sm** show crystallographic symmetry with the metal atoms, the amido nitrogen atom N1, a further nitrogen atom of the Me_3TACD ligand, as well as the central carbon atoms of both allyl ligands in the mirror plane (Figure 3, center). All complexes show a shorter distance between the metal and the amido nitrogen atom Ln–N1 (≈2.3 Å) than to the other three amine nitrogen atoms (mean interatomic distance of 2.7 Å). The Me_3TACD ligand is highly distorted due to the sp^2 amido nitrogen atom (sum of the C-N-C and C-N-Ln angles, see Table 1) and the resulting coplanar orientation of the five atoms (C-C-N(sp^2)-C-C) around the amido nitrogen atom.[7a] The decreasing ionic radius on going from **1-La** to **1-Y** results in an increasing bend of the ring ligand and migration of the metal towards the cavity of the ligand. On the one hand, the distance between the N_4-plane and the metal center decreases even more with the ionic radii (Table 1) than expected from the lanthanide contraction. On the other hand, the hole size measured in the complexes (Table 1) hardly varies with the ionic radii of the lanthanides and is on average 0.06 Å larger than in the hydrochloric salt.

Although the solid-state structures of **1-Y**, **1-Pr**, and **1-Sm** show disorder within the allyl group or the Me_3TACD fragment, the disorder could be modeled well with split posi-

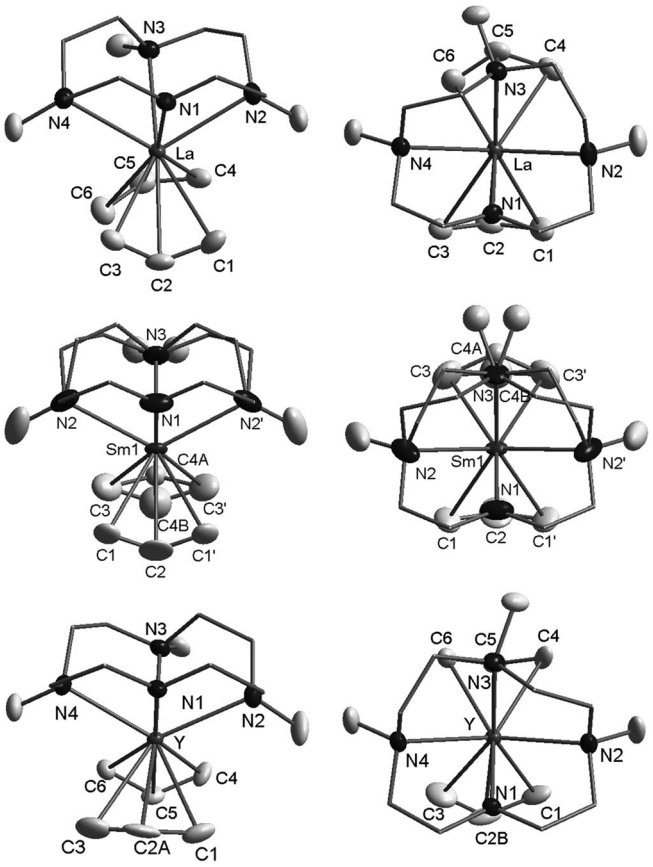

Figure 3. Molecular structures of **1-La** (top), **1-Sm** (center), and **1-Y** (bottom). Thermal ellipsoids are drawn at the 50% probability level. Hydrogen atoms are omitted for clarity. The disordered carbon atom positions in **1-Y** are shown with only one split position.

tions for the carbon atoms. The crystal structure of **1-La**, which does not show any disorder, differs from **1-Y**, **1-Sm**, and **1-Pr** by a paddle-wheel-like arrangement of the allyl groups. In **1-La** the *trans*-located allyl ligand (relative to the amido nitrogen atom) shows slightly elongated La–C bonds (mean value of 2.87 Å ranging from 2.791(4) to 2.918(4) Å in *trans* versus 2.83 Å ranging from 2.808(4) to 2.859(4) Å in *cis*) and a larger C-C-C angle ($\theta_{trans}=128.7(4)$ vs. $\theta_{cis}=127.6(4)°$). While the allyl group *cis* to the amido nitrogen atom shows a symmetrical coordination to the metal center, the *trans*-located allyl group is displaced by the *trans* influence[16] induced by the amido donor.

The dynamic behavior of **1-La** in [D_8]toluene solution was investigated by ^{1}H NMR spectroscopy in the temperature range of −80 to +80 °C (Figure 4). At +80 °C, the spectrum shows high symmetry. The signal assigned to the methane protons at around $\delta=6.40$ ppm shows one emerging quintet ($^3J(H,H)=12.0$ Hz) for both allyl groups located *cis* and *trans* relative to the amido nitrogen atom. The simple high-temperature NMR spectrum may be explained by a C_s-symmetric structure that results from a dynamic exchange of the *cis*-/*trans*-allyl groups. This process may involve twisting of the square antiprismatic coordination geometry by rotating the allyl groups with the C2/C5 methine carbon atoms moving below N2/N4 through a cubic transition state. Another process indicated by the broadening of the resonances at 3.06 ($^3J(H,H)=8.3$ Hz, *syn*) and 2.82 ppm ($^3J(H,H)=15.1$ Hz, *anti*) is the onset of exchange between *syn*- and *anti*-protons through σ–π rearrangement, without reaching coalescence. At 0 °C the coalescence of the signals for the *cis*- and *trans*-located allyl ligands is observed as one broad signal for the terminal protons ranging from $\delta=2.75$ to 3.50 ppm. Correspondingly a broad signal at $\delta=6.52$ ppm

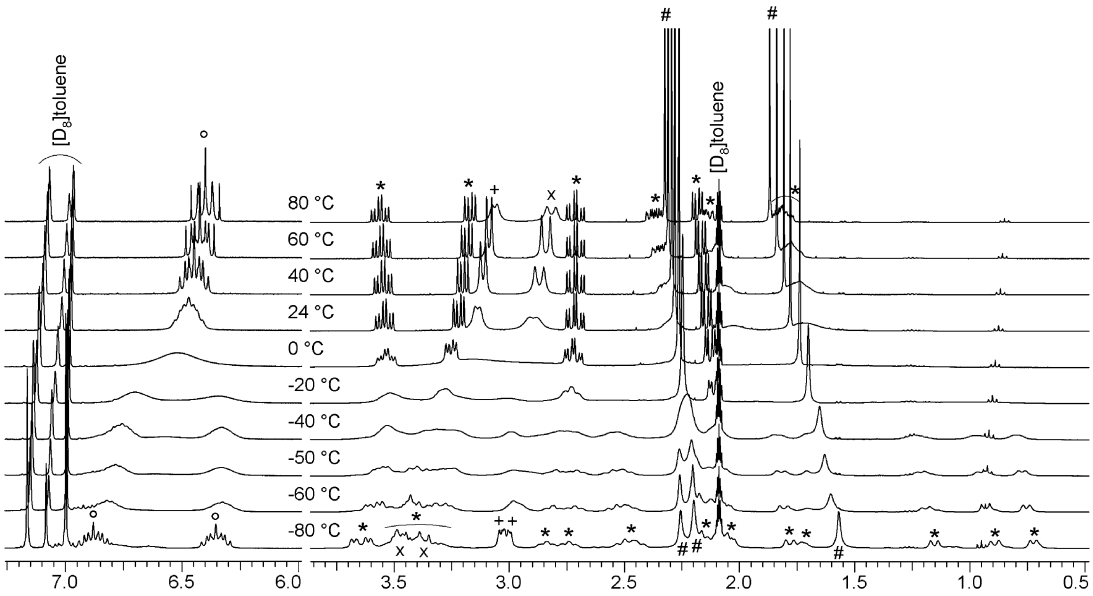

Figure 4. Variable-temperature ^{1}H NMR spectra of **1-La** in [D_8]toluene from −80 to +80 °C. The left-hand side shows the methine protons (°) of the two allyl groups. The right-hand side shows the *syn*- (+) and *anti*-protons (×) as well as the CH_2CH_2 resonances (*) and the methyl groups (#) of the Me_3TACD ligand.

Table 1. Selected interatomic distances [Å] and angles [°] of [Ln(Me_3TACD)(η^3-C_3H_5)$_2$] (Ln = La **1-La**, Pr **1-Pr**, Sm **1-Sm**, Y **1-Y**), [Ce(Me_3TACD)(η^3-C_3H_5)(thf)$_2$][BPh_4] (**2-Ce**), and [La(Me_3TACD)(μ-H)$_2$]$_4$ (**3-La**).

	1-La	**1-Y**		**1-Pr**	**1-Sm**		**2-Ce**		**3-La**
Ln−C1	2.808(4)	2.641(3)	Ln−C1	2.782(5)	2.743(3)	Ce−C1	2.822(3)	La1−La2	3.9154(4)
Ln−C2	2.859(4)	2.684(4)* 2.610(8)*	Ln−C2	2.751(7)	2.700(5)	Ce−C2	2.816(3)	La1−La3	3.8912(6)
Ln−C3	2.837(4)	2.754(4)	–	–	–	Ce−C3	2.792(3)	La1−La4	4.1544(4)
C1−C2	1.388(6)	1.245(11)* 1.442(7)*	C1−C2	1.341(6)	1.337(4)	C1−C2	1.376(5)	La2−La3	3.8916(5)
C2−C3	1.373(6)	1.376(13)* 1.260(6)*	–	–	–	C2−C3	1.376(5)	La2−La4	4.1161(5)
C1-C2-C3	127.6(4)	131.1(5) 139.6(9)	C1-C2-C1′	132.8(10)	134.1(7)	C1-C2-C3	127.1(3)	La3−La4	4.1689(4)
Ln−C4	2.791(4)	2.740(3)	Ln−C3	2.744(5)	2.716(3)	–	–	La4-H8-H7	174(2)
Ln−C5	2.918(4)	2.698(3)	Ln−C4	2.824(14)* 2.83(2)*	2.779(9)* 2.758(15)*	–	–	–	–
Ln−C6	2.887(4)	2.697(3)	–	–	–	–	–	La1···(N_4-plane)	1.7783(15)
C4−C5	1.386(6)	1.381(4)	C3−C4	1.284(10)* 1.344(9)*	1.341(6)* 1.291(6)*	–	–	*r*	2.085(3)
C5−C6	1.374(6)	1.375(4)	–	–	–	–	–	*r*(H)	1.365(3)
C4-C5-C6	128.7(4)	127.8(3)	C3-C4-C3′	128.6(13)* 141(3)*	131.0(9)* 141.8(14)*	–	–	Σ(C-N1-La1/C)	357.1
Ln−N1	2.404(3)	2.239(2)	Ln−N1	2.312(6)	2.291(4)	Ce−N1	2.312(2)	La2···(N_4-plane)	1.7659(15)
Ln−N2	2.715(3)	2.567(2)	Ln−N2	2.680(5)	2.628(3)	Ce−N2	2.699(2)	*r*	2.026(3)
Ln−N3	2.743(3)	2.632(2)	Ln−N3	2.702(5)	2.653(3)	Ce−N3	2.772(2)	*r*(H)	1.306(3)
Ln−N4	2.703(3)	2.578(2)	–	–	–	Ce−N4	2.710(2)	Σ(C-N1-La2/C)	359.3
N1-Ln-N3	85.68(9)	88.84(8)	N1-Ln-N3	86.1(2)	87.30(13)	N1-Ce-N3	85.98(8)	La3···(N_4-plane)	1.7723(16)
N1−N3	3.509(4)	3.420(3)	N1−N3	3.433(9)	3.423(5)	N1−N3	3.483(3)	*r*	2.069(3)
N2-Ln-N4	116.31(9)	123.28(7)	N2-Ln-N2′	119.5(3)	121.58(14)	N2-Ce-N4	116.81(7)	*r*(H)	1.349(3)
N2−N4	4.602(4)	4.527(3)	N2−N2′	4.631(12)	4.588(6)	N2−N4	4.607(3)	Σ(C-N1-La3/C)	358.6
Ln···(N_4-plane)	1.6491(15)	1.4681(12)	Ln···(N_4-plane)	1.579(8)	1.5250(19)	Ce···(N_4-plane)	1.6190(13)	La4···(N_4-plane)	1.7833(15)
r[13a]	2.041(2)	2.005(3)	*r*	2.031(3)	2.020(2)	*r*	2.035(3)	*r*	2.026(3)
r(H)[13a]	1.321(2)	1.285(3)	*r*(H)	1.311(3)	1.300(2)	*r*(H)	1.315(3)	*r*(H)	1.306(3)
Σ(C-N1-Ln/C)	357.4	359.3	Σ(C-N1-Ln/C)	359.0	358.9	Σ(C-N1-Ce/C)	358.6	Σ(C-N1-La4/C)	358.9

[*] These atoms are disordered and could be modeled with split positions.

shows the coalescence of the methine protons, which splits into one signal for each allyl ligand at −20 °C. The free energy of activation $\Delta G^{\neq} = 52.74\ kJ\,mol^{-1}$ at the estimated coalescence temperature of 0 °C was calculated using the Eyring equation. As consequence of nonequivalent *cis*- and *trans*-allyl groups, two sets of η^3-bonded allyl signals are found at −80 °C. Over the entire temperature range, the allyl ligands retain the η^3-binding mode on the NMR timescale. The Me_3TACD ligand displays eight diagnostic signals for the four CH_2CH_2 groups at 80 °C, which indicates the rapid exchange process between the two macrocyclic ring conformations [(λδδδ) and (δλλλ)] on the NMR timescale.[7a] Lowering the temperature to −20 °C results in the broadening of all ring resonances. At −50 °C, the signals of the CH_2CH_2 groups split into two sets of signals to become distinct at −80 °C. Above −40 °C, the three methyl groups of the Me_3TACD ligand show two singlets of intensity ratio 1:2, consistent with C_s-symmetry of the ring caused by a dynamic exchange process in solution. Below −40 °C, three distinct singlets are detected, in agreement with the asymmetric structure found in the solid state (Figure 3, top).

The compounds **1-Ce**, **1-Pr**, **1-Nd**, and **1-Sm** display a net broadening and a paramagnetically induced dispersion of all the signals in the ^{1}H NMR spectra. The magnitude varies in the order **1-Sm** < **1-Ce** < **1-Nd** < **1-Pr** with signals ranging from −110 to 120 ppm for **1-Pr** (Figure 5). In particular, the

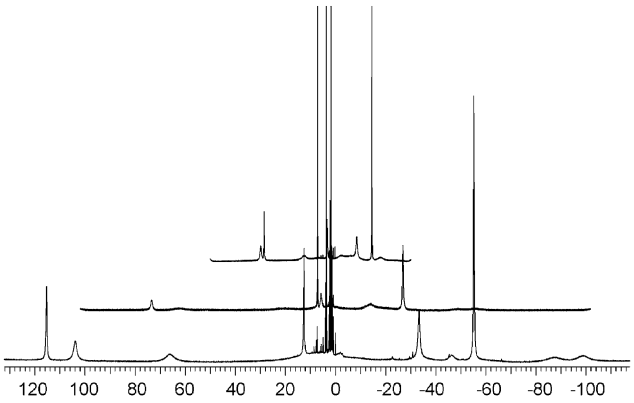

Figure 5. ^{1}H NMR spectra of the paramagnetic complexes: from top to bottom **1-Ce**, **1-Nd**, and **1-Pr** in [D_6]benzene.

syn- and *anti*-signals and those of the CH_2CH_2 bridges are so broad that assignment and integration are difficult. At room temperature, C_s-symmetry on the NMR timescale is found for **1-Ce**, **1-Nd**, and **1-Pr**, indicated by nine resonances in the ^{1}H NMR spectrum.

Cationic mono(allyl) complexes: Reaction of **1-La**, **1-Ce**, and **1-Nd** with [NEt_3H][$B(C_6X_5)_4$] (X = H, F) led to com-

plexes $[Ln(Me_3TACD)(\eta^3\text{-}C_3H_5)(thf)_2][B(C_6X_5)_4]$ (X = H, Ln = La **2-La**, Ce **2-Ce**, Nd **2-Nd**; X = F, Ln = La **2^F-La**) (Scheme 2). Compounds **2-La**, **2-Ce**, and **2-Nd** are barely soluble in THF but ^1H, $^{13}C\{^1H\}$, and ^{11}B NMR spectra could be obtained. The ^1H NMR spectrum of **2-La** shows a sharp triplet of triplets at $\delta = 6.16$ ppm for the methine proton and at $\delta = 2.94$ and 2.26 ppm two distinct doublets for *syn*- ($^3J(H,H) = 9.3$ Hz) and *anti*-protons ($^3J(H,H) = 15.6$ Hz). The four CH_2CH_2 signals have a similar shape to those in the neutral compound **1-La**. The ^{11}B NMR spectrum of **2-La** displays one signal at $\delta = -6.5$ ppm, consistent with the presence of a single compound. The ^1H NMR spectra of the paramagnetic analogues **2-Ce** and **2-Nd** differ from those of the neutral precursors. In contrast to the proton signals of the cation that are spread over a large range of chemical shifts, the proton signals of the borate anions appear like in **2-La** at around $\delta = 6.0$ ppm, thus pointing out that no interactions between metal center and anion are found in THF solution.

The solid-state structure of the cation **2-Ce** was investigated to understand the effects of the cationic metal center (Figure 6). The compound crystallizes as an ion pair without close interactions between the cation and anion.[17] The unit cell contains a cocrystallized THF molecule disordered around a center of symmetry in the lattice. The geometry around the metal center is best described by a three-legged piano stool in which the carbon atom C2 of the allyl moiety as well as the atoms O1 and O2 of the coordinating thf molecules build the three legs and the rhombic base is formed by the four nitrogen atoms of the ligand scaffold. The allyl ligand is located *trans* to the amido nitrogen atom and shows an η^3-binding mode. This is confirmed by similar Ce–C_{allyl} contacts (Ce1–C1 2.822(3), Ce1–C2 2.816(3), and Ce1–C3 2.792(3) Å) as well as equal C–C bond lengths of 1.376(5) Å (for C1–C2 and C2–C3). The two thf molecules that coordinate to the metal center show interatomic Ce1–O_{thf} distances of 2.596(2) and 2.641(2) Å, which are within the expected range. The Me_3TACD ligand binds to the metal center in the same way as in the neutral compounds. The calculated Ce1···N_4-plane distance of 1.6190(13) Å and hole size in **2-Ce** ($r(H) = 1.315(3)$ Å)[13a] fit between the values measured in the neutral compounds **1-La** and **1-Pr**. The comparison of the neutral and cationic compounds in the solid state does not reveal any difference caused by the higher Lewis acidity of the metal center in the cationic analogue **2-Ce**, as found between $[Ce(\eta^3\text{-}C_3H_5)_3(thf)_3]$ and $[Ce(\eta^3\text{-}C_3H_5)_2(thf)_4][BPh_4]$.[15d]

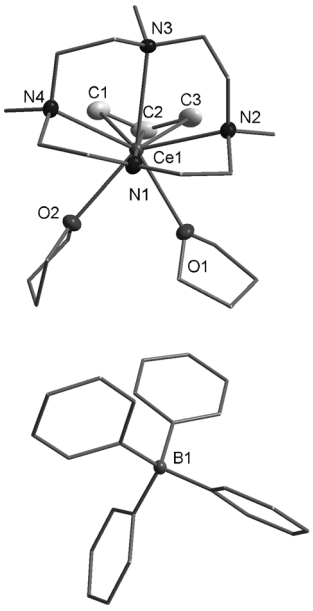

Figure 6. Molecular structure of the cationic part of $[Ce(Me_3TACD)(\eta^3\text{-}C_3H_5)(thf)_2][B(C_6H_5)_4]$ (**2-Ce**). Thermal ellipsoids are drawn at the 50% probability level. Hydrogen atoms are omitted for clarity.

To enhance the solubility of the cation, $[La(Me_3TACD)(\eta^3\text{-}C_3H_5)(thf)_2][B(C_6F_5)_4]$ (**2^F-La**) was synthesized with the Brønsted acid dimethylanilinium tetrakis(pentafluorophenyl)borate. **2^F-La** provides the same cation as **2-La** combined with a fluorinated anion $[B(C_6F_5)_4]^-$, which makes the compound more soluble in less polar solvents such as benzene.[17]

Dihydrido complexes: The bis(trimethylsilylmethyl) complexes $[Ln(Me_3TACD)(CH_2SiMe_3)_2]$ (Ln = Y, Ho, Lu) were reported to react with phenylsilane to form the hydrido complexes $[Ln(Me_3TACD)H_2]_3$.[7a] **1-La** and **1-Sm** underwent hydrogenolysis to give the corresponding dihydrido complexes $[Ln(Me_3TACD)H_2]_n$ (Ln = La **3-La**, $n = 4$; Ln = Sm **3-Sm**; Scheme 2). The formation of the hydrido compounds took three days at 50 °C and was monitored by ^1H NMR spectroscopy. The ^1H NMR spectrum in $[D_8]$THF shows a single compound **3-La** with a broad singlet at $\delta = 10.53$ ppm, assigned to the lanthanum hydride, five signals for the CH_2CH_2 protons, and two singlets for the terminal methyl groups of the Me_3TACD ligand.

X-ray diffraction quality crystals of **3-La** were grown from a benzene solution at 5 °C. The solid-state structure of **3-La** contains one molecule of benzene in the lattice and does not show any disorder, thereby allowing the location of all hydride positions (Figure 7). Molecular lanthanum hydrides are rare,[18] **3-La** representing the first example of structurally characterized non-cyclopentadienyl-supported lanthanum hydride. The solid-state structure shows a tetrameric La_4H_8 core (Figure 8), which contains six μ-bridging hydrides on the edges, one face-capped μ_3-hydride, and one μ_4-hydride in the center, coordinated tetrahedrally by four lanthanum atoms ($\theta = 104$–$116°$). The structure of the tetrameric core corresponds to the Ln_4H_8 core found in $[(TpMe_2)LnH_2]_4$[19] (Ln = Y, Sm, Yb, Lu) and in the cyclopentadienyl (Cp)-supported La_4H_8 cluster.[20] The lanthanum compound **3-La** differs from the highly symmetric trinuclear cluster $[Y(Me_3TACD)(\mu\text{-}H)_2]_3$[7a] (**3-Y**) that contains only μ-hydrides. In **3-La**, C_3-symmetry is found for the La_4H_8 core with a the μ_3-bonded H7, the central μ_4-H8, and La4 located on the (noncrystallographic) C_3-axis. Atoms La1, La2, and La3 form a pseudo-hexagonal plane with H1, H2, and H3; each

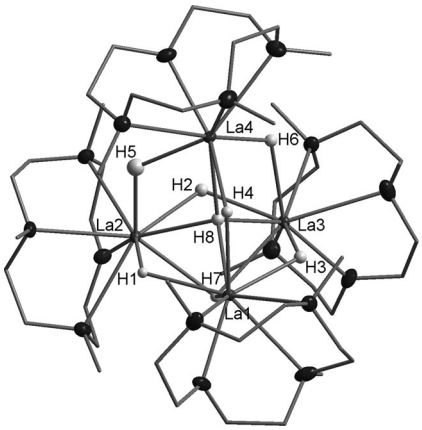

Figure 7. Molecular structure of $[La_4(Me_3TACD)_4(\mu\text{-}H)_6(\mu_3\text{-}H)(\mu_4\text{-}H)]$ (**3-La**). Thermal ellipsoids are drawn at the 50% probability level. Hydrogen atoms of the Me_3TACD ligand are omitted for clarity.

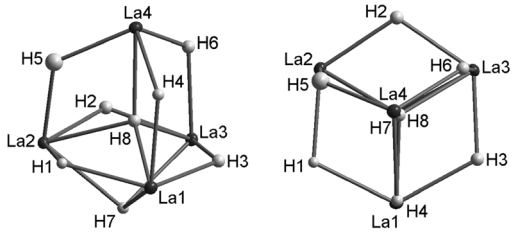

Figure 8. Side (left) and top view (right) of the La_4H_8 core of **3-La**.

lanthanum atom is nine-coordinated in square-antiprism geometry by four nitrogen atoms and four hydrogen atoms additionally capped by the hydride ligand H8. La4 is eight-coordinated in a piano-stool-like manner with also one additional hydride ligand H8. The La···La contacts between the lanthanum atoms situated in the pseudo-hexagonal plane are longer than those predicted for $[Cp_4La_4H_8]$ (La···La = 3.866 Å[20] vs. La1···La2 = 3.9154(4), La2···La3 = 3.8916(5), and La1···La3 = 3.8912(6) Å). The distances between La(1–3) and La4, which is located on the C_3-axis, are ≈0.2 Å longer (La1···La4 = 4.1544(4), La2···La4 = 4.1161(5), and La3···La4 = 4.1689(4) Å) which is also longer than those predicted by calculation for $[Cp_4La_4H_8]$ (La···La = 4.054 Å[20]). All La–N distances are longer than in the bis(allyl) compound **1-La**; the La···N_4-plane distances are 0.1 Å longer (La1···N_4-plane = 1.7783(15), La2···N_4-plane = 1.7659(15), La3···N_4-plane = 1.7723(16), and La4···N_4-plane = 1.7833(15) Å).

The ^{1}H NMR spectrum of **3-Sm** shows lower symmetry than **3-La** in $[D_8]$THF solution with seven signals for the CH_2CH_2 and two for the methyl groups. The line broadening precludes the observation of the hydrido signal in **3-Sm**. The previously reported yttrium hydrido compound prepared from $[Y(Me_3TACD)(CH_2SiMe_3)_2]$ was also obtained from **1-Y**. The ^{1}H and $^{13}C\{^1H\}$ NMR spectra were identical to those of the reported trinuclear dihydride $[Y(Me_3TACD)(\mu\text{-}H)_2]_3$ (**3-Y**).[7a] These observations confirm that allyl ligands are suitable precursors for the generation of hydrido compounds and provide an alternative to the commonly used CH_2SiMe_3 ligand.

Reduction of furfural: Conversion of furfural with phenylsilane by using catalytic amounts (2.5 mol%) of $[Y(Me_3TACD)(CH_2SiMe_3)_2]$ (**4-Y**),[7a] **1-La**, or **3-Y** was monitored by ^{1}H NMR spectroscopy. Within 7 min, the 1,2-addition products furfuryl silanolates were produced (Scheme 3). Only bis(furfuryl)phenylsilane (**A**) and tris(furfuryl)phenylsilane (**B**), commonly difficult to access due to steric hindrance,[21] were detected (Table 2). Monofurfuryl(phenyl)silane, which was formed in the first step, is favored and disappeared immediately under formation of **A** and **B** (Table 2, **1-La**, 67% **A** and 33% **B**). After three days the concentration of **B** increased, thus indicating a metal-mediated redistribution reaction. At lower concentrations of **1-La** ([**1-La**]:furfural = 1:80), the reaction reached full conversion within 20 min. At low catalyst loadings (1:500) 13% conversion was already observed after 30 min. The hydride **3-Y** appears to be the most active, because 87% of **B** was already detected after a reaction time of 7 min (Table 2). In all cases, the GC-MS analysis shows 2-furfuryl alcohol (**C**) as the only final product. The side products disiloxanes or enoxysilanes that are usually observed in the hydrosilylation of aldehydes[21] were not detected. The few examples of hydrosilylation of furfural reported in the literature use nickel or iron catalysts that require 20 h to achieve high conversions.[22,23]

As organolanthanides are known to be active catalysts in the hydrogenation of simple alkenes,[24] the scope of the catalyst system was explored in the hydrogenation of furfural

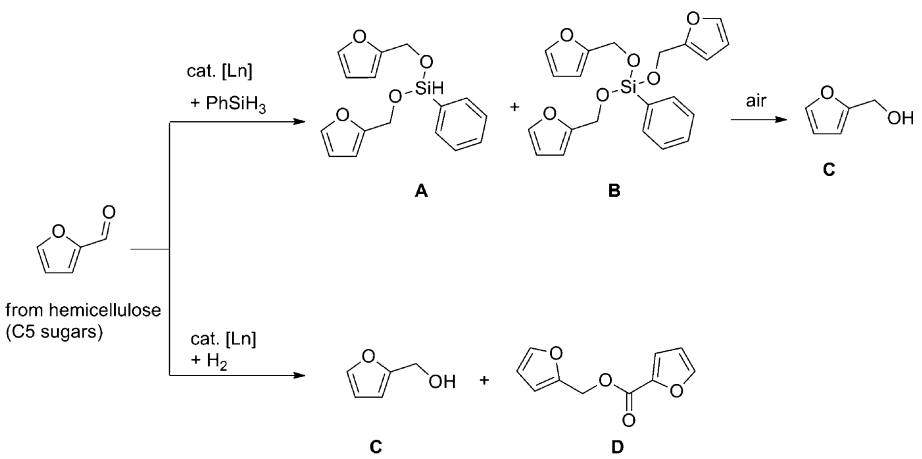

Scheme 3. Conversion of furfural into 2-furfuryl alcohol (**C**) and furfuryl 2-furoate (**D**).

Table 2. Hydrosilylation of furfural catalyzed by [Y(Me_3TACD)-(CH_2SiMe_3)$_2$] (**4-Y**), [Y(Me_3TACD)(μ-H_2)]$_3$ (**3-Y**), and [La(Me_3TACD)-(η^3-C_3H_5)$_2$] (**1-La**).[a]

Complex	Complex:furfural	Time	Conversion [%]	Product ratio A	B
4-Y[b]	1:40	<7 min	>98	81	19
1-La[b]	1:40	<7 min	>98	67	33
		3 days	>98	31	69
1-La[c]	1:80	3 min	67	n.d.	n.d.
		20 min	98	n.d.	n.d.
1-La[d]	1:500	30 min	13	n.d.	n.d.
3-Y[b]	1:40	<7 min	>98	18	82

[a] $PhSiH_3$ (1.25 equiv). [b] [D_6]benzene (0.6 mL), 25 °C, **A**:**B** ratio determined by ^{1}H NMR before workup. [c] **1-La** (20 mg), toluene (1 mL), GC-MS analysis of a sample (0.1 mL) mixed with wet acetone (3 mL). [d] **1-La** (5 mg), furfural (414 μL). n.d. = not detected.

with molecular hydrogen. Whereas the catalytic hydrosilylation of furfural led only to 2-furfuryl alcohol (**C**), the hydrogenation of furfural at a metal to furfural ratio of 1:40 led to a mixture of **C** and furfuryl 2-furoate (**D**) in low yield (Scheme 3, Table 3). The formation of **D** does not depend

Table 3. Hydrogenation of furfural catalyzed by [Y(Me_3TACD)-(CH_2SiMe_3)$_2$] (**4-Y**) and [Ln(Me_3TACD)(η^3-C_3H_5)$_2$] (Ln = La, **1-La**; Ce, **1-Ce**) at different overall concentrations.[a]

Complex	c[furfural] [mol L^{-1}]	Time [days]	Conversion [%]	Product ratio C	D
1-La	1.0	6	29	64	36
1-Ce	1.0	6	14	86	14
4-Y[b]	1.0	6	17	89	11
4-Y[b]	0.5	6	11	89	11

[a] Complex:furfural 1:40, [D_8]THF (0.6 mL), $p(H_2)$ = 5 bar, 50 °C. [b] About 6% of unidentified byproduct detected by ^{1}H NMR spectroscopy and GC-MS (*m*/*z* 188).

on the concentration of the in situ formed **3-Y**,[7a] but the total yield increases at higher concentration. The highest conversion was found for **1-La** but **4-Y** showed the highest selectivity towards the furfuryl alcohol **C**. The experiments show that the catalytic hydrogenation of furfural is possible, but no full conversion was attained under the conditions investigated.

In ^{1}H NMR experiments in [D_8]THF, furfural was treated with **3-Y** in varying ratios (**3-Y**:furfural = 1:2, 1:4, 1:8, 1:12) without additional hydrogen. After eight days at 25 °C at ratios of 1:2, 1:4, and 1:8, signals attributed to **C** and **D** were found by GC-MS analysis, whereas in ^{1}H NMR spectra **D** and broad signals attributed to an yttrium furfuryl alkoxide species as well as other byproducts are found. At a ratio of 1:12, ^{1}H NMR spectra also show the presence of **C** besides **D** and the yttrium furfuryl alkoxide species.

Hydrogenation of furan and 2-methylfuran: The conversions of furan and 2-methylfuran in the presence of hydrogen and **1-Y**, **1-La**, **1-Ce**, **1-Nd**, or **1-Sm** lead to the corresponding alkenes and alkanes (Table 4). This reaction is formally a hydrodeoxygenation, which involves the removal of oxygen (Scheme 4).[25] The C–O bond activation of ether, essential for this type of reaction, is known to be induced by metallo-

Table 4. Hydrodeoxygenation of 2-methylfuran induced by **1-Y**, **1-La**, **1-Ce**, **1-Nd**, **1-Sm**, or **3-La**.[a]

Complex	Solvent	Substrate R	Conversion [%]	Products [%][b] alkene	alkane
1-La	[D_6]benzene	Me	60	52	n.d.
1-Ce	[D_6]benzene	Me	57	42	n.d.
1-Nd	[D_6]benzene	Me	53	37	n.d.
1-Sm	[D_6]benzene	Me	38	70	n.d.
1-Y	[D_6]benzene	Me	43	98	n.d.
1-La	[D_6]benzene	H	61	33	n.d.
3-La[c]	[D_8]THF	Me	17	51	26
1-La	[D_8]THF	Me	68	40	n.d.
1-Sm	[D_8]THF	Me	72	72	n.d.

[a] Complex:substrate 1:1, c(complex) = 0.09 mol L^{-1}, solvent (0.5 mL), $p(H_2)$ = 5.5 bar, time = 6 days. [b] R = Me, F: *cis*-/*trans*-2-pentene, G: *n*-pentane; R = H, H: *cis*-/*trans*-2-butene, I: *n*-butane. [c] c(complex) = 0.18 mol L^{-1}. n.d. = not detected.

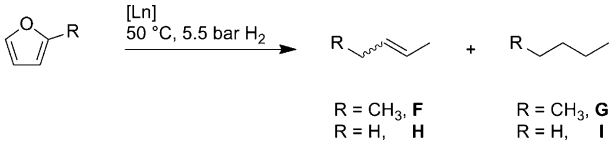

Scheme 4. Hydrodeoxygenation of furan and 2-methylfuran induced by **1-Y**, **1-La**, **1-Ce**, **1-Nd**, and **1-Sm**.

cene hydrides and half-sandwich alkyls of rare-earth metals.[26] Teuben et al. reported [Cp*$_2$YH$_2$]-mediated hydrodeoxygenation of furan leading to the formation of *n*-butane and dimeric oxo-yttriocene [(Cp*$_2$Y)$_2$(μ-O)].[26a]

The activity and selectivity in the hydrodeoxygenation of 2-methylfuran was investigated in [D_6]benzene and [D_8]THF as well as with different metal complexes **1-Y**, **1-La**, **1-Ce**, **1-Nd** , and **1-Sm** (Scheme 4, Table 4). The highest activity in [D_6]benzene is observed with **1-La** and can further be increased by using [D_8]THF. In contrast, the selectivity towards the formation of *cis*/*trans*-2-pentene (**F**) decreases with the metal size. This indicates that with larger metals further hydrogenation to *n*-pentane (**G**) occurs, which is found in the reaction with **3-La**.[27] Kinetic investigations show that the substitution pattern of furan also has an influence on the activity, indicating an α activation of the furan ring mediated by the metal center (Figure 9).[28] This activation was further investigated by deuteration experiments.

Treatment of furan derivatives with D_2 and using stoichiometric amounts of metal complex was performed to reveal the regioselectivity during the hydrodeoxygenation. In the conversion of furan in the presence of **1-Y**, after 22 h all peaks assigned to furan protons disappeared in the ^{1}H NMR spectrum. The GC-MS chromatogram of the solution showed two signals, attributed to [D_7–D_8]2-butene (*m*/*z* 64) and [D_3–D_4]furan. The presence of [D_3–D_4]furan indicates a metal-mediated H/D scrambling of the protons in the α and

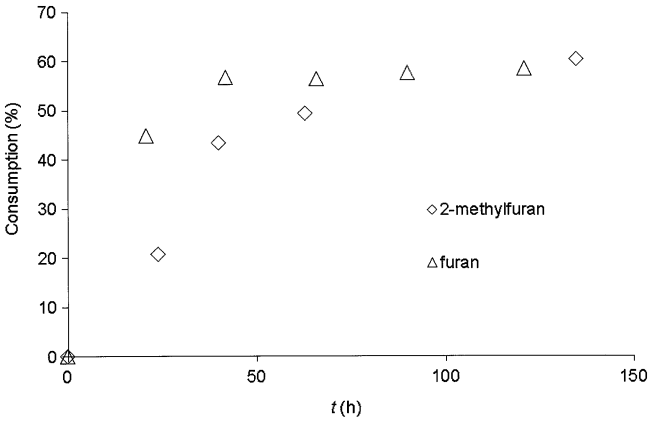

Figure 9. Conversion of furan and 2-methylfuran with **1-La** in [D_6]benzene.

β positions. In the conversion of 2-methylfuran with **1-Y**, beyond [D_0–D_{10}]2-pentene also α- and β-H/D exchange leading mainly to [D_2]2-methylfuran is found by ^{1}H NMR spectroscopy and GC-MS analysis. With larger metals **1-La** and **1-Sm**, conversion to [D_0–D_{10}]2-pentene and deuteration of the α proton in 2-methylfuran were observed. In an experiment with **1-La** performed over 60 h, the signal assigned to the α proton disappeared and the complete transition of the β-H signal from a multiplet to a doublet indicates an H/D exchange mainly in the α position (Figure 10). These results were confirmed by GC-MS analysis, in which lower amounts of [D_2]2-methylfuran were detected compared to the reaction with **1-Y**.

For the hydrodeoxygenation of 2-methylfuran at ambient pressure with [La(Me_3TACD)D_2] (**3^D-La**) without addition of D_2, two signals corresponding to [D_1–D_5]2-pentene and [D_0]2-methylfuran were found by GC-MS. Thus, the scrambling induced by the H/D exchange only takes place in the presence of excess D_2.

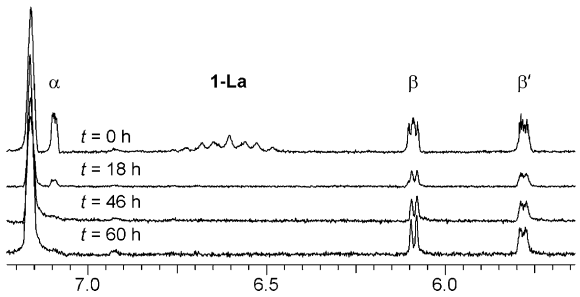

Figure 10. Deuteration of 2-methylfuran in the presence of **1-La** performed in [D_6]benzene at 50 °C analyzed by ^{1}H NMR spectroscopy at the start of the reaction, and after 18, 46, and 60 h.

Conclusion

The synthesis of the proligand (Me_3TACD)H (**L**H) was improved as a two-step reaction starting from the commercially available cyclen. Tris(allyl) complexes are suitable precursors for thermally stable allyl complexes supported by a Me_3TACD ligand [Ln(Me_3TACD)(η^3-C_3H_5)$_2$] (Ln = Y **1-Y**, La **1-La**, Nd **1-Nd**, Ce **1-Ce**, Pr **1-Pr**, Sm **1-Sm**). These bis(allyl) compounds display two η^3-bonded allyl fragments in the solid state as well as in solution. Protonolysis by Brønsted acids generates allyl cations as solvent-separated ion pairs [Ln(Me_3TACD)(η^3-C_3H_5)(thf)$_2$] [B(C_6X_5)$_4$] (X = H, Ln = La **2-La**, Ce **2-Ce**, Nd **2-Nd**; X = F, La **2^F-La**). Allyl complexes of the lighter lanthanides are suitable precursors for the synthesis of hydrido compounds [Ln(Me_3TACD)H_2]$_n$ (Ln = Y **3-Y**, n = 3;[7a] Ln = La **3-La**, n = 4; Ln = Sm **3-Sm**), thus providing an alternative to the commonly used CH_2SiMe_3 complexes. [La_4(Me_3TACD)$_4$(μ-H)$_6$(μ_3-H)(μ_4-H)] (**3-La**) is the first example of a structurally characterized non-cyclopentadienyl-supported lanthanum hydride. A tetrameric La_4H_8 core is found in the solid-state structure with one μ^4-hydride ligand in the center. The nuclearity of the hydrido cluster with a Me_3TACD ligand thus depends on the metal size.

The complexes [Ln(Me_3TACD)R_2] (R = η^3-C_3H_5, Ln = La **1-La**, Y **1-Y**; R = H, Ln = Y **3-Y**; R = CH_2SiMe_3, Ln = Y **4-Y**) catalyzed the hydrosilylation of furfural and hydrogenation to the corresponding alcohol or furfuryl 2-furoate. The active species in these reactions is presumably the dihydride complex [Ln(Me_3TACD)H_2]$_n$ (Ln = Y **3-Y**, La **3-La**) formed by hydrogenation of the neutral bis(allyl) moiety. Hydrodeoxygenation of furan and 2-methylfuran leading to the formation of olefins and alkanes was observed by using [Ln(Me_3TACD)(R)$_2$] (R = η^3-C_3H_5, Ln = Y **1-Y**, La **1-La**, Ce **1-Ce** , Pr **1-Pr**, Nd **1-Nd**, Sm **1-Sm**; R = H, Ln = La **3-La**).

Experimental Section

General considerations: All operations were performed under an inert atmosphere of argon by using standard Schlenk-line or glovebox techniques. THF, toluene, 1,4-dioxane, furan, 2-methylfuran, 2,5-dimethylfuran, deuterated THF, and benzene were dried over sodium benzophenone ketyl. *n*-Pentane was dried over sodium benzophenone ketyl/triglyme. $PhSiH_3$ was dried over sodium. The following compounds were prepared according to published procedures: 1,4,7-triformylcyclen,[11] [Y(Me_3TACD)(CH_2SiMe_3)$_2$] (**4-Y**),[7a] [Ln(η^3-C_3H_5)$_3$(1,4-dioxane)] (Ln = Y, La, Ce, Pr, Nd, Sm),[15] [Nd(η^3-C_3H_5)$_2$(thf)$_3$][B(C_6H_5)$_4$].[15d] All other chemicals were commercially available and used after appropriate purification. NMR spectra were recorded on a Varian Mercury 200BB spectrometer, on a Bruker DRX 400 spectrometer (^{1}H 400.1 MHz, ^{13}C{^{1}H} 100.6 MHz) or on a Varian Unity 500 spectrometer (^{1}H 499.6 MHz, ^{13}C{^{1}H} 125.6 MHz). All chemical shifts are given in ppm and were referenced internally by using the residual solvent resonances and reported relative to $SiMe_4$. For GC-MS analysis, the filtered reaction solution was analyzed by a Shimadzu GCMS-QP2010 Plus instrument run on helium as carrier gas.

Single-crystal X-ray diffraction measurements were performed on a Bruker AXS diffractometer equipped with an Incoatec microsource and an APEX area detector using $Mo_{K\alpha}$ radiation. Experimental parameters and refinement results are given in Table 5. The data reductions were performed with the Bruker SAINT software.[29a] Absorption corrections were carried out by using the program SADABS or Mulabs as implemented in the program system Platon.[29b,c] The structures were solved by direct methods using the program SIR-92,[29d] except for the structure of **1-Pr** that was solved by isotypic replacement using the coordinates of

Table 5. Crystallographic data for complexes **L**H·HCl, **1-La**, **1-Pr**, **1-Sm**, **1-Y**, **2-Ce**, and **3-La**.

Compound	**L**H·HCl	**1-La**	**1-Pr**	**1-Sm**	**1-Y**	**2-Ce**	**3-La**
empirical formula	$C_{23}H_{56}C_{l4}N_8$	$C_{17}H_{35}LaN_4$	$C_{17}H_{35}N_4Pr$	$C_{17}H_{35}N_4Sm$	$C_{17}H_{35}N_4Y$	$C_{96}H_{140}B_2Ce_2N_8O_5$	$C_{50}H_{114}La_4N_{16}$
M_r [g mol^{-1}]	586.56	434.40	436.40	445.84	384.40	1788.02	1495.20
crystal size [mm]	0.20×0.08×0.08	0.14×0.08×0.05	0.12×0.08×0.05	0.22×0.06×0.06	0.34×0.28×0.17	0.23×0.20×0.18	0.45×0.41×0.30
crystal color and habit	colorless rod	colorless block	grey block	orange block	yellow rod	colorless block	yellow block
crystal system	orthorhombic	orthorhombic	tetragonal	tetragonal	monoclinic	triclinic	orthorhombic
space group	*Pbcn*	*Pccn*	$P4_2/mbc$	$P4_2/mbc$	$P2_1/n$	$P\bar{1}$	$P2_12_12_1$
a [Å]	15.147(3)	19.173(3)	18.8913(18)	18.7546(3)	8.7065(15)	9.1271(5)	12.9291(15)
b [Å]	19.473(4)	13.896(2)	18.8913(18)	18.7546(3)	13.856(2)	14.6650(7)	22.025(3)
c [Å]	10.882(2)	14.715(2)	11.1454(11)	11.1890(4)	15.723(3)	17.1018(9)	22.570(3)
α [°]	90.00	90.00	90.00	90.00	90.00	76.9905(8)	90.00
β [°]	90.00	90.00	90.00	90.00	94.028(3)	84.5358(8)	90.00
γ [°]	90.00	90.00	90.00	90.00	90.00	86.7703(8)	90.00
V [Å^3]	3209.7(11)	3920.5(10)	3977.6(7)	3935.56(17)	1892.1(6)	2218.7(2)	6427.1(14)
Z	4	8	8	8	4	1	4
ρ_{calcd} [g cm^{-3}]	1.214	1.472	1.457	1.505	1.349	1.338	1.545
T [K]	100(2)	130(2)	130(2)	130(2)	100(2)	130(2)	100(2)
$\mu(Mo_{K\alpha})$ [mm^{-1}]	0.395	2.183	2.453	2.987	3.086	1.069	2.649
$F(000)$	1272	1776	1792	1816	816	938	3015
θ range [°]	2.53–21.44	1.81–30.66	2.41–30.60	2.42–28.12	2.60–29.83	1.23–30.78	1.82–30.10
hkl indices	±15, ±19, ±11	±27, ±19, ±20	−25–14, ±26, −14–15	±24, ±24, ±14	±12, ±19, −22–21	−13–12, ±20, ±23	±17, −29–30, ±31
number of refl. collected	22501	52604	28176	50632	27370	32916	91538
number of refl. observed ($I>2\sigma(I)$)	1425	4100	2057	2025	3499	9773	16789
number of ind. refl. (R_{int})	1821 (0.1159)	5803 (0.0806)	3105 (0.1306)	2520 (0.0806)	5376 (0.0846)	12570 (0.0464)	17520 (0.0604)
data/rest./par.	1821/0/174	5803/0/242	3105/0/105	2520/0/108	5376/0/241	12570/0/507	17520/0/675
R_1, wR_2 ($I>2\sigma(I)$)	0.0398, 0.0937	0.0339, 0.0690	0.0471, 0.0904	0.0256, 0.0569	0.0393, 0.0817	0.0355, 0.0760	0.0263, 0.0569
R_1, wR_2 (all data)	0.0527, 0.988	0.0638, 0.0871	0.0867, 0.1029	0.0350, 0.0587	0.0788, 0.0952	0.0491, 0.0955	0.0283, 0.0577
goodness-of-fit on F^2	1.026	1.100	0.950	0.963	1.007	0.970	1.036
largest diff. in peak and hole [e Å^{-3}]	0.217, −0.302	2.225, −1.499	1.027, −1.518	0.925, −0.575	0.555, −0.493	1.660, −1.070	1.004, −0.858

1-Sm. All refinements were carried out by the full-matrix least-squares method using SHELXL-97 as implemented in the WinGX program system.[29e,f] The structures of **1-Pr**, **1-Sm**, and **1-Y** show disordered positions for several carbon atoms within one allyl ligand and the Me_3TACD ring. The disorder was modeled by using split positions for the carbon atoms. Compound **2-Ce** crystallized with an additional solvent molecule of THF in the lattice. The hydrogen atoms were included in idealized positions, except for the position of H1 in **L**H·HCl, the hydrogen atoms within the allyl ligands in **1-La**, as well as the hydride atoms in **3-La** (H1–H8) that were refined in their positions. The graphical representations in the Figures were performed with the program DIAMOND.[29g] CCDC-833281 (**L**H·HCl), CCDC-833282 (**1-La**), CCDC-833283 (**1-Pr**), CCDC-833284 (**1-Sm**), CCDC-833285 (**1-Y**), CCDC-83328 (**2-Ce**), and CCDC-833287 (**3-La**) contain the supplementary crystallographic data for this paper. These data can be obtained free of charge from The Cambridge Crystallographic Data Centre via www.ccdc.cam.ac.uk/data_request/cif.

[Me_3TACD]H (LH): 1,4,7-Triformylcyclen (806 mg, 3.145 mmol) was treated with a solution of [BH_3(thf)] in THF (50 mL, 1.0 M) and stirred for 72 h with heating at reflux. Water (10 mL) was added at 0 °C and, after removal of the volatiles at reduced pressure, the afforded colorless powder was treated with hydrochloric acid (50 mL, 2.0 M) and heated at reflux for 2 h. The volatiles were removed to give colorless microcrystals, which were dissolved in water. The solution was filtered through an anion-exchange resin (DOWEX-1×8–200, OH^-) affording a viscous colorless oil (480 mg, 2.237 mmol, 71 %). ^{1}H NMR ([D_1]chloroform, 25 °C): δ = 2.14 (s, 3H; CH_3), 2.16 (s, 6H; CH_3), 2.27 (m, 8H; CH_2), 2.30–2.37 (m, 4H; CH_2), 2.48–2.57 ppm (m, 4H; CH_2), signal for NH not detected; ^{13}C{^{1}H} NMR ([D_1]chloroform, 25 °C): δ = 43.5 (CH_3), 44.5 (CH_3), 45.6 (CH_2), 53.4 (CH_2), 55.0 (CH_2), 55.1 ppm (CH_2); elemental analysis calcd (%) for $C_{11}H_{26}N_4$ (M = 214.35 g mol^{-1}): C 61.64, H 12.23, N 26.14; found: C 61.15, H 12.39, N 25.75; X-ray diffraction quality crystals of the hydrochloride **L**H·HCl were obtained from the hydrochloric acid solution of the crude mixture and subsequent neutralization with NaOH to pH 13, followed by extraction with dichloromethane and crystallization from a saturated dichloromethane solution.

[La(Me_3TACD)(η^3-C_3H_5)$_2$] (1-La): A solution of **L**H (214 mg, 1.00 mmol) in THF (5 mL) was added dropwise to a solution of [La(η^3-C_3H_5)$_3$(1,4-dioxane)] (350 mg, 1.00 mmol) in THF (5 mL). The resulting mixture was stirred for 2 h, filtered, and dried under reduced pressure. The resulting solid was washed with *n*-pentane (4×3 mL) and dried to give **1-La** as a colorless powder (387 mg, 90 %). ^{1}H NMR ([D_6]benzene, 25 °C): δ = 1.69 (br m, 4H; CH_2), 1.74 (s, 3H; CH_3), 1.99 (br s, 2H; CH_2), 2.14 (dd, ^2J(H,H) = 11.8, ^3J(H,H) = 4.3 Hz, 2H; CH_2), 2.26 (s, 6H; CH_3), 2.28 (br s, 2H; CH_2), 2.75 (td, ^2J(H,H) = ^3J(H,H) = 12.5 Hz, ^3J(H,H) = 4.8 Hz, 2H; CH_2), 3.03 (d, ^3J(H,H) = 13.3 Hz, 4H; *anti*-CH_2CHCH_2), 3.26 (d, ^3J(H,H) = 8.7 Hz, 4H; *syn*-CH_2CHCH_2), 3.29 (dd, ^2J(H,H) = 12.3, ^3J(H,H) = 5.5 Hz, 2H; CH_2), 3.56 (td, ^2J(H,H) = ^3J(H,H) = 12.3 Hz, ^3J(H,H) = 5.5 Hz, 2H; CH_2), 6.60 ppm (tt, ^3J(H,H) = 13.3, ^3J(H,H) = 8.7 Hz,

2H; CH_2CHCH_2); ^{1}H NMR ([D$_8$]THF, 25 °C): δ = 2.36 (s, 3H; CH_3), 2.37–2.47 (br s, 4H; CH_2), 2.50 (dd, ^2J(H,H) = 11.8, ^3J(H,H) = 4.5 Hz, 2H; CH_2), 2.54 (bd, 4H; CH_2CHCH_2), 2.59–2.67 (br s, 2H; CH_2), 2.63 (s, 6H; CH_3), 2.79 (bd, 4H; CH_2CHCH_2), 2.81–2.92 (br s, 2H; CH_2), 2.88 (td, ^2J(H,H) = ^3J(H,H) = 12.4 Hz, ^3J(H,H) = 4.7 Hz, 2H; CH_2), 3.13 (dd, ^2J(H,H) = 12.3, ^3J(H,H) = 5.6 Hz, 2H; CH_2), 3.64 (td, ^2J(H,H) = ^3J(H,H) = 12.1 Hz, ^3J(H,H) = 5.6 Hz, 2H; CH_2), 6.13 ppm (m, 2H; CH_2CHCH_2); ^{1}H NMR ([D$_8$]toluene, 80 °C): δ = 1.75–1.88 (m, 4H; CH_2), 1.87 (s, 3H; CH_3), 2.11–2.18 (m, 2H; CH_2), 2.18 (dd, ^2J(H,H) = 11.8, ^3J(H,H) = 4.8 Hz, 2H; CH_2), 2.33 (s, 6H; CH_3), 2.31–2.40 (m, 2H; CH_2), 2.71 (td, ^2J(H,H) = ^3J(H,H) = 12.3 Hz, ^3J(H,H) = 4.8 Hz, 2H; CH_2), 2.82 (bd, ^3J(H,H) = 15.1 Hz, 4H; *anti*-CH_2CHCH_2), 3.06 (bd, ^3J(H,H) = 8.3 Hz, 4H; *syn*-CH_2CHCH_2), 3.17 (dd, ^2J(H,H) = 12.6, ^3J(H,H) = 5.8 Hz, 2H; CH_2), 3.56 (td, ^2J(H,H) = ^3J(H,H) = 12.0 Hz, ^3J(H,H) = 5.8 Hz, 2H; CH_2), 6.40 ppm ("quint", ^3J(H,H) = 12.0 Hz, 2H; CH_2CHCH_2); ^{1}H NMR ([D$_8$]toluene, −80 °C): δ = 0.72 (d, ^3J(H,H) = 10.3 Hz, 1H; CH_2), 0.89 (d, ^3J(H,H) = 14.6 Hz, 1H; CH_2), 1.15 (d, ^3J(H,H) = 12.8 Hz, 1H; CH_2), 1.57 (s, 3H; CH_3), 1.72 (bd, ^3J(H,H) = 6.3 Hz, 1H; CH_2), 1.78 (d, ^3J(H,H) = 13.6 Hz, 1H; CH_2), 1.98–2.17 (m, 3H; CH_2), 2.20 (s, 3H; CH_3), 2.26 (s, 3H; CH_3), 2.48 (m, 2H; CH_2), 2.74 (m, 1H; CH_2), 2.83 (m, 1H; CH_2), 2.98–3.06 (m, 4H; CH_2CHCH_2), 3.18–3.56 (m, 2H; CH_2), 3.37 (d, ^3J(H,H) = 15.3 Hz, 2H; CH_2CHCH_2), 3.47 (d, ^3J(H,H) = 15.3 Hz, 2H; CH_2CHCH_2), 3.61 (d, ^3J(H,H) = 8.5 Hz, 1H; CH_2), 3.66 (d, ^3J(H,H) = 8.3 Hz, 1H; CH_2), 6.35 (tt, ^3J(H,H) = 15.3, ^3J(H,H) = 9.3 Hz, 1H; CH_2CHCH_2), 6.88 ppm (tt, ^3J(H,H) = 15.3, ^3J(H,H) = 9.0 Hz, 1H; CH_2CHCH_2); ^{13}C{^{1}H} NMR ([D$_6$]benzene, 25 °C): δ = 45.7 (CH_3), 48.5 (CH_3), 52.5 (CH_2), 56.0 (CH_2), 56.2 (CH_2), 62.1 (CH_2), 71.0 (CH_2CHCH_2), 148.0 ppm (CH_2CHCH_2); ^{13}C{^{1}H} NMR ([D$_8$]THF, 25 °C): δ = 46.3 (CH_3), 49.0 (CH_3), 53.5 (CH_2), 56.7 (CH_2), 57.2 (CH_2), 62.9 (CH_2), 70.5 (CH_2CHCH_2), 148.1 ppm (CH_2CHCH_2); elemental analysis calcd (%) for $C_{17}H_{35}LaN_4$ (M = 434.40 g mol^{-1}): C 47.00, H 8.12, N 12.90; found: C 46.94, H 8.04, N 12.85.

[Ce(Me$_3$TACD)(η^3-C$_3$H$_5$)$_2$] (1-Ce): A solution of **L**H (214 mg, 1.00 mmol) in THF (5 mL) was added dropwise to a solution of [Ce(η^3-C_3H_5)$_3$(1,4-dioxane)] (351 mg, 1.00 mmol) in THF (5 mL). The resulting solution was stirred for 2 h, filtered, and dried under reduced pressure. The resulting solid was washed with *n*-pentane (4×3 mL) and dried to give an orange powder (328.5 mg, 75 %). ^{1}H NMR ([D$_6$]benzene, 25 °C): δ = −17.90 (br s), −14.44 (s), −8.38 (br s), −5.80 (br s), −2.08 (br s), 3.27 (m), 12.64 (br s), 28.50 (br s), 29.95 ppm (br s); ^{13}C{^{1}H} NMR ([D$_6$]benzene, 25 °C): δ = 11.3 (CH_3), 23.7 (CH_3), 34.7 (CH_2), 35.4 (CH_2), 56.2 (CH_2), 84.4 ppm (CH_2), allyl signal could not be detected; elemental analysis calcd (%) for $C_{17}H_{35}N_4Ce$ (M = 435.61 g mol^{-1}): C 46.87, H 8.10, N 12.86; found: C 47.09, H 7.83, N 12.72.

[Pr(Me$_3$TACD)(η^3-C$_3$H$_5$)$_2$] (1-Pr): A solution of **L**H (64 mg, 0.30 mmol) in THF (5 mL) was added dropwise to a solution of [Pr(η^3-C_3H_5)$_3$(1,4-dioxane)] (106 mg, 0.30 mmol) in THF (5 mL). The resulting solution was stirred for 2 h, filtered, and dried under reduced pressure. The resulting solid was washed with *n*-pentane (4×3 mL) and dried to give a pale green powder (52 mg, 40 %). ^{1}H NMR ([D$_6$]benzene, 25 °C): δ = −97.2, −87.2, −54.6, −45.5, −33.5, 12.1, 65.9, 103.9, 115.4 ppm; ^{13}C{^{1}H} NMR ([D$_6$]benzene, 25 °C): δ = −70.4, −53.4, −30.2, −27.0, 74.8, 112.6, 192.5 ppm; elemental analysis calcd (%) for $C_{17}H_{35}N_4Pr$ (M = 435.61 g mol^{-1}): C 46.79, H 8.10, N 12.84; found: C 44.12, H 7.05, N 12.97.

[Nd(Me$_3$TACD)(η^3-C$_3$H$_5$)$_2$] (1-Nd): A solution of **L**H (214 mg, 1.00 mmol) in THF (2 mL) was added dropwise to a solution of [Nd(η^3-C_3H_5)$_3$(1,4-dioxane)] (356 mg, 1.00 mmol) in THF (2 mL). The resulting solution was stirred for 2 h, filtered, and dried under reduced pressure. The resulting solid was washed with *n*-pentane and dried to give a green powder (286 mg, 57 %). ^{1}H NMR ([D$_8$]THF, 25 °C): δ = −56.78 (br s), −49.78 (br s), −27.37 (br s), −16.86 (br s), −13.48 (br s), 6.47 (br s), 20.72 (br s), 63.59 (br s), 74.57 ppm (br s); ^{13}C{^{1}H} NMR ([D$_8$]THF, 25 °C): δ = −41.6, −10.5, −0.8, 0.2, 32.6, 67.4, 76.5, 267.7 ppm; elemental analysis calcd (%) for $C_{17}H_{35}N_4Nd$ (M = 439.73 g mol^{-1}): C 46.43, H 8.02, N 12.74; found: C 41.93, H 7.77, N 12.83.

[Sm(Me$_3$TACD)(η^3-C$_3$H$_5$)$_2$] (1-Sm): A solution of [Sm(η^3-C_3H_5)$_3$(1,4-dioxane)] (600 mg, 1.66 mmol) in THF (10 mL) was treated with a solution of **L**H (355 mg, 1.66 mmol) in THF (3 mL). After stirring for 2 h, the solvent was removed under reduced pressure and the remaining product was dissolved in a toluene/*n*-pentane mixture. Cooling at −30 °C gave **1-Sm** (700 mg, 95 %) as orange crystals. ^{1}H NMR ([D$_6$]benzene, 25 °C): δ = −0.70 (br s; CH_3), −0.06 (br s; CH_2), 0.41 (br s; CH_2), 0.57 (br s; CH_3), 2.74 (br s; CH_2), 2.88 (br s; CH_2), 3.65 (br s; CH_2), 4.34 (br s; CH_2), 5.55 (br s; CH_2CHCH_2), 7.57 (br s; CH_2CHCH_2) 11.82 ppm (br s; CH_2CHCH_2); ^{13}C{^{1}H} NMR ([D$_6$]benzene, 25 °C): δ = 40.9 (CH_2), 41.9 (CH_2), 44.6 (CH_3), 51.2 (CH_3), 54.8 (CH_2), 57.4 (CH_2), 66.7 (CH_2), 67.8 (CH_2), 149.8 (CH), 161.1 ppm (CH_2); elemental analysis calcd (%) for $C_{17}H_{35}N_4Sm$ (M = 445.85 g mol^{-1}): C 45.80, H 7.91, N 12.57, Sm 33.72; found: C 43.74, H 7.41, N 12.93, Sm 32.8.

[Y(Me$_3$TACD)(η^3-C$_3$H$_5$)$_2$] (1-Y): A solution of [Y(η^3-C_3H_5)$_3$(1,4-dioxane)] (300 mg, 1.00 mmol) in THF (10 mL) was treated with a solution of **L**H (214 mg, 1.00 mmol) in THF (3 mL). After stirring for 2 h, the solvent was removed under reduced pressure and the remaining solid was dissolved in a toluene/*n*-pentane mixture. Cooling at −30 °C gave **1-Y** (280 mg, 73 %) as yellow crystals. ^{1}H NMR ([D$_6$]benzene, 25 °C): δ = 1.76 (s, 3H; CH_3), 1.80–1.47 (br m, 4H; CH_2), 2.09 (dd, ^2J(H,H) = 11.5, ^3J(H,H) = 5.5 Hz, 2H; CH_2), 2.23 (s, 6H; CH_3), 2.31–2.21 (br s, 4H; CH_2), 2.79 (td, ^2J(H,H) = ^3J(H,H) = 12.3 Hz, ^3J(H,H) = 6.3 Hz, 2H; CH_2), 2.69–2.96 (br s, 4H; *anti*-CH_2CHCH_2), 3.22 (dd, ^2J(H,H) = 12.0, ^3J(H,H) = 6.5 Hz, 2H; CH_2), 3.01–3.47 (br s, 4H; *syn*-CH_2CHCH_2), 3.59 (td, ^2J(H,H) = ^3J(H,H) = 11.8 Hz, ^3J(H,H) = 6.3 Hz, 2H; CH_2), 6.88 ppm (br s, 2H; CH_2CHCH_2); ^{13}C{^{1}H} NMR ([D$_6$]benzene, 25 °C): δ = 46.8 (CH_3), 50.2 (CH_3), 53.1 (CH_2), 55.3 (CH_2), 56.3 (CH_2), 63.0 (CH_2), 64.9 (CH_2CHCH_2), 66.7 (CH_2CHCH_2), 150.2 ppm (CH_2CHCH_2); elemental analysis calcd (%) for $C_{17}H_{35}N_4Y$ (M = 384.40 g mol^{-1}): C 53.12, H 9.18, N 14.58, Y 23.13; found: C 51.56, H 9.05, N 14.42, Y 23.2.

[La(Me$_3$TACD)(η^3-C$_3$H$_5$)(thf)$_2$][B(C$_6$H$_5$)$_4$] (2-La): A solution of **1-La** (87 mg, 0.20 mmol) in THF (2.5 mL) was treated with a solution of [NEt_3H][B(C_6H_5)$_4$] (84 mg, 0.20 mmol) in THF (2.5 mL). After stirring for 1.5 h, the solvent was removed under reduced pressure and the remaining product was washed with *n*-pentane (4×2.5 mL) to afford **2-La** (149 mg, 0.158 mmol, 79 %) as a colorless powder. ^{1}H NMR ([D$_8$]THF, 25 °C): δ = 1.78 (m, 8H; β-thf), 2.26 (d, ^3J(H,H) = 15.6 Hz, 2H; *anti*-CH_2CHCH_2), 2.06 (br s, 2H; CH_2), 2.25–2.62 (br s, 4H; CH_2), 2.35 (s, 3H; CH_3), 2.53 (s, 6H; CH_3), 2.56 (dd, ^2J(H,H) = 12.5, ^3J(H,H) = 4.8 Hz, 2H; CH_2), 2.86 (td, ^2J(H,H) = ^3J(H,H) = 12.6 Hz, ^3J(H,H) = 4.8 Hz, 4H; CH_2), 2.94 (d, ^3J(H,H) = 9.3 Hz, 2H; *syn*-CH_2CHCH_2), 3.13 (dd, ^2J(H,H) = 12.8, ^3J(H,H) = 5.4 Hz, 2H; CH_2), 3.22 (td, ^2J(H,H) = ^3J(H,H) = 12.5 Hz, ^3J(H,H) = 5.2 Hz, 2H; CH_2), 3.62 (m, 8H; α-thf), 6.16 (tt, ^3J(H,H) = 9.3, ^3J(H,H) = 15.6 Hz, 1H; CH_2CHCH_2), 6.72 (t, ^3J(H,H) = 7.3 Hz, 4H; *p*-Ph), 6.86 (t, ^3J(H,H) = 7.5 Hz, 8H; *m*-Ph), 7.28 ppm (m, 8H; *o*-Ph); ^{13}C{^{1}H} NMR ([D$_8$]THF, 25 °C): δ = 26.4 (β-thf), 46.9 (CH_3), 48.5 (CH_3), 53.7 (CH_2), 55.6 (CH_2), 56.9 (CH_2), 61.4 (CH_2), 68.2 (α-thf), 75.1 (CH_2CHCH_2), 121.9 (*p*-Ph), 125.7 (*m*-Ph), 137.2 (*o*-Ph), 149.2 (CH_2CHCH_2), 165.2 ppm (quart, ^1J(B,C) = 49.3 Hz; *i*-Ph); ^{11}B{^{1}H} NMR ([D$_8$]THF, 25 °C): δ = −4.70 ppm; elemental analysis calcd (%) for $C_{46}H_{66}N_4BLaN_4O_2$ (M = 856.43 g mol^{-1}): C 64.49, H 7.76, N 6.54; found: C 58.89, H 6.24, N 7.32.

[La(Me$_3$TACD)(η^3-C$_3$H$_5$)(thf)$_2$][B(C$_6$F$_5$)$_4$] (2^F-La): A solution of [$HNMe_2Ph$][B(C_6F_5)$_4$] (160 mg, 0.2 mL) in THF (2.5 mL) was added dropwise to a solution of **1-La** (87 mg, 0.20 mmol) in THF (2.5 mL) and the mixture was stirred for 1.5 h. All volatiles were removed under reduced pressure. The resulting light brown powder was washed with *n*-pentane (4×3 mL) and dried under reduced pressure to afford **2^F-La** (221 mg, 90 %). ^{1}H NMR ([D$_8$]THF, 25 °C):δ = 1.77 (m, 8H; β-thf), 2.30 (d, ^3J(H,H) = 15.6 Hz, 2H; *anti*-CH_2CHCH_2), 2.47 (s, 3H; CH_3), 2.54 (dd, ^2J(H,H) = 12.8, ^3J(H,H) = 5.0 Hz, 2H; CH_2), 2.43–2.72 (br m, 6H; CH_2), 2.62 (s, 6H; CH_3), 2.90 (td, ^2J(H,H) = ^3J(H,H) = 12.8 Hz, ^3J(H,H) = 4.9 Hz, 2H; CH_2), 2.97 (d, ^3J(H,H) = 9.0 Hz, 2H; *syn*-CH_2CHCH_2), 3.01 (m, 2H; CH_2), 3.15 (dd, ^2J(H,H) = 13.0, ^3J(H,H) = 5.4 Hz, 2H; CH_2), 3.31 (td, ^2J(H,H) = ^3J(H,H) = 12.6 Hz, ^3J(H,H) = 5.4 Hz, 2H; CH_2), 3.62 (m, 8H; α-thf), 6.20 ppm (tt, ^3J(H,H) = 15.5, ^3J(H,H) = 9.2 Hz, 1H; CH_2CHCH_2); ^{13}C{^{1}H} NMR ([D$_8$]THF, 25 °C): δ = 26.5 (β-thf), 47.1 (CH_3), 48.6 (CH_3), 54.0 (CH_2), 55.7 (CH_2), 57.2 (CH_2), 61.6 (CH_2), 68.4 (CH_2, α-thf), 75.5 (CH_2CHCH_2), 125.5 (br m; *i*-Ph), 137.3 (d, ^1J(CF) =

245.4 Hz; *m*-Ph), 139.3 (d, ^1J(CF) = 242.8 Hz; *p*-Ph), 149.3 (d, ^1J(CF) = 241.9 Hz; *o*-Ph), 149.5 ppm (CH_2CHCH_2).

[Ce(Me$_3$TACD)(η^3-C$_3$H$_5$)(thf)$_2$][B(C$_6$H$_5$)$_4$] (2-Ce): A solution of **1-Ce** (87 mg, 0.20 mmol) in THF (2.5 mL) was treated with a solution of [NEt_3H][$B(C_6H_5)_4$] (84 mg, 0.20 mmol) in THF (2.5 mL). After stirring for 0.5 h, the solvent was removed under reduced pressure and the remaining product was washed with *n*-pentane (5×2.5 mL) to afford **2-Ce** (144 mg, 0.157 mmol, 79%) as a yellow powder. Diffraction-quality crystals of **2-Ce** were obtained from an *n*-pentane/THF mixture at −40 °C. ^{1}H NMR ([D$_8$]THF, 25 °C): δ = −18.03, −17.83, −8.75–3.24, 0.91, 1.34, 1.79, 3.62, 6.58, 6.84, 7.91, 9.91, 14.80, 22.92, 36.48, 45.92, 66.15 ppm; ^{13}C{^{1}H} NMR ([D$_8$]THF, 25 °C): δ = 11.8 (CH_3), 23.2 (CH_3), 26.3 (β-thf), 31.6 (CH_2), 35.1 (CH_2), 37.3 (CH_2), 54.6 (CH_2), 68.2 (α-thf), 121.5 (*p*-Ph), 125.3 (quart, ^3J(B,C) = 2.6 Hz; *m*-Ph), 137.2 (m, ^2J(B,C) = 1.7 Hz; *o*-Ph), 165.2 ppm (quart, ^1J(B,C) = 49.3 Hz; *i*-Ph) (allyl signals were not detected). ^{11}B{^{1}H} NMR ([D$_8$]THF, 25 °C): δ = −7.03 ppm; elemental analysis calcd (%) for $C_{46}H_{66}N_4BCeN_4O_2$ (M = 857.43 g mol^{-1}): C 64.40, H 7.75, N 6.53; found: C 59.04, H 7.34, N 7.13.

[Nd(Me$_3$TACD)(η^3-C$_3$H$_5$)(thf)$_2$][B(C$_6$H$_5$)$_4$] (2-Nd): A THF (2 mL) solution of **L**H (28 mg, 0.13 mmol) was added to a solution of [$Nd(\eta^3$-$C_3H_5)_2$-$(thf)_3$][$B(C_6H_5)_4$] (100 mg, 0.13 mmol) in THF (2 mL). The reaction mixture was stirred for 1.5 h, then all volatiles were removed under reduced pressure to afford **2-Nd** as a light green powder (75 mg, 0.08 mmol, 61%). ^{1}H NMR ([D$_8$]THF, 25 °C): δ = −42.27 (br s), −31.14 (br s), 1.83 (m; β-thf), 3.63 (m; α-thf), 5.78 + 6.26 (2× br s; *o*-Ph + *m*-Ph), 6.48 (br s; *p*-Ph), 16.51 (br s), 51.14 ppm (br s); ^{13}C{^{1}H} NMR ([D$_8$]THF, 25 °C): δ = 26.5 (β-thf), 68.2 (α-thf), 121.2 (*p*-Ph), 124.87 (*m*-Ph), 135.9 (*o*-Ph), 163.7 ppm (quart, ^1J(B,C) = 49.4 Hz; *i*-Ph) (allyl signals were not detected); elemental analysis calcd (%) for $C_{42}H_{58}BN_4NdO$ (M = 1579.98 g mol^{-1}): C 64.69, H 6.85, N 6.56; found: C 59.58, H 7.01, N 6.84.

[Y(Me$_3$TACD)(μ-H)$_2$]$_3$ (3-Y): [D$_8$]THF (0.5 mL) was added to **1-Y** (40 mg, 0.104 mmol) in a Teflon-screw-top pressure NMR tube (Wilmad). The NMR tube was cooled with liquid nitrogen, connected to a Schlenk line, and evacuated. The NMR tube was then warmed to room temperature and after the solution had melted, pressurized with hydrogen (p(H$_2$) = 5 bar) and placed into an oil bath at 50 °C. The conversion was followed by ^{1}H NMR spectroscopy for three days. ^{1}H NMR ([D$_6$]benzene, 25 °C): δ = 2.09 (m, 2H; CH_2), 2.27 (m, 4H; CH_2); 2.47 (dd, ^2J(H,H) = 10.7, ^3J(H,H) = 4.3 Hz, 2H; CH_2), 2.62 (m, 2H; CH_2), 2.65 (s, 3H; CH_3), 2.84 (s, 6H; CH_3), 3.20 (ddd, ^2J(H,H) = 12.1, ^3J(H,H) = 11.8, ^3J(H,H) = 4.3 Hz, 2H; CH_2), 3.46 (dd, ^2J(H,H) = 11.7, ^3J(H,H) = 5.6 Hz, 2H; CH_2), 3.90 (m, 2H; CH_2), 6.45 ppm (m, 2H; YH); ^{13}C{^{1}H} NMR ([D$_6$]benzene, 25 °C) δ = 46.3 (CH_3), 50.1 (CH_3), 52.3 (CH_2), 56.3 (CH_2), 57.1 (CH_2), 63.3 ppm (CH_2); elemental analysis calcd (%) for $C_{99}H_{241}N_{36}Y_3$ (M = 912.79 g mol^{-1}): C 43.42, H 8.94, N 18.41; found: C 43.99, H 7.93, N 16.37.

[La$_4$(Me$_3$TACD)$_4$(μ-H)$_6$(μ$_3$-H)(μ$_4$-H)] (3-La): [D$_8$]THF (0.5 mL) was added to **1-La** (40 mg, 0.092 mmol) in a Teflon-screw-top pressure NMR tube (Wilmad). The NMR tube was cooled with liquid nitrogen, connected to a Schlenk line, and evacuated. The NMR tube was then warmed to room temperature and after the solution had melted, pressurized with hydrogen (p(H$_2$) = 5 bar) and placed into an oil bath at 50 °C. The conversion was followed by ^{1}H NMR spectroscopy for three days. ^{1}H NMR ([D$_8$]THF, 25 °C): δ = 2.21 (m, 4H; CH_2), 2.54 (br s, 4H; CH_2), 2.63 (s, 3H; CH_3), 2.78 (m, 4H; CH_2), 2.79 (s, 6H; CH_3), 2.99 (m, 2H; CH_2), 3.39 (m, 2H; CH_2), 10.52 ppm (br s, 2H; LaH); ^{13}C{^{1}H} NMR ([D$_8$]THF, 25 °C): δ = 45.2 (CH_3), 49.0 (CH_3), 52.8 (CH_2), 56.6 (CH_2), 57.1 (CH_2), 60.8 ppm (CH_2). X-ray diffraction quality crystals of **3-La** were collected after reaction of **1-La** (169 mg, 0.40 mmol) with $PhSiH_3$ (63 mg, 0.58 mmol) for 1 h in benzene at RT, followed by cooling of the reaction mixture over one week at 5 °C.

[La(Me$_3$TACD)D$_2$] (3^D-La): This compound was prepared following the same procedure as for **3-La** but using D_2.

[Sm(Me$_3$TACD)H$_2$] (3-Sm): [D$_8$]THF (0.5 mL) was added to **1-Sm** (18 mg, 0.04 mmol) in a Teflon-screw-top pressure NMR tube (Wilmad). The NMR tube was cooled with liquid nitrogen, connected to a Schlenk line, and evacuated. The NMR tube was then warmed to room temperature and after the solution had melted, pressurized with hydrogen (p(H$_2$) = 5 bar) and placed into an oil bath at 50 °C. The conversion was followed by ^{1}H NMR for three days. ^{1}H NMR ([D$_8$]THF, 25 °C): δ = −4.58 (s, 6H; CH_3), 0.30 (m, 2H; CH_2), 1.24 (m, 2H; CH_2), 1.76 (m, 2H; CH_2), 4.03 (m, 4H; CH_2), 5.22 (s, 3H; CH_3), 6.08 (m, 2H; CH_2), 6.18 (m, 2H; CH_2), 6.68 ppm (m, 2H; CH_2); ^{13}C{^{1}H} NMR ([D$_8$]THF, 25 °C): δ = 41.4 (CH_3), 51.3 (CH_3), 53.3 (CH_2), 61.2 (CH_2), 63.4 (CH_2). 68.9 ppm ($CH)_2$.

Typical procedure for the hydrodeoxygenation of furanics: a) [D$_8$]THF or [D$_6$]benzene (0.5 mL) was added to complex **1-Y**, **1-La**, **1-Ce**, **1-Nd**, or **1-Sm** (0.045 mmol) in a Teflon-screw-top pressure NMR tube (Wilmad). After dissolution of all solid, furan (3.4 μL, 0.045 mmol), 2-methylfuran (4.1 μL, 0.045 mmol), or 2,5-dimethylfuran (4.9 μL, 0.045 mmol) was added. The NMR tube was cooled with liquid nitrogen, connected to a Schlenk-line, and evacuated. The NMR tube was then warmed to room temperature and after the solution had melted, pressurized with hydrogen (p(H$_2$) = 5.5 bar) and placed into an oil bath at 50 °C. b) Alternative procedure with prior hydrogenation of **1-La** to **3-La**: [D$_8$]THF (0.5 mL) was added to complex **1-La** (0.045 mmol) in a Teflon-screw-top pressure NMR tube (Wilmad). The NMR tube was cooled with liquid nitrogen, connected to a Schlenk line, and evacuated. The NMR tube was then warmed to room temperature and after the solution had melted, pressurized with hydrogen (p(H$_2$) = 5.5 bar) and placed into an oil bath at 50 °C for three days. All solvents were then removed under reduced pressure. After dissolution of all solid in [D$_8$]THF (0.5 mL), 2-methylfuran (7 μL, 0.092 mmol) was added. The NMR tube was cooled with liquid nitrogen, connected to a Schlenk-line, and evacuated. The NMR tube was then warmed to room temperature and after the solution had melted, pressurized with hydrogen (5.5 bar), placed into an oil bath at 50 °C for 22 days, and removed from the oil bath every day for ^{1}H NMR measurement.

2-Pentene: MS: *m*/*z* (%): 70 (38) [M^+], 55 (100) [M^+-CH_3]; *cis*-2-pentene: ^{1}H NMR ([D$_8$]THF, 25 °C): δ = 0.94 (t, ^3J(H,H) = 7.3 Hz, 3H; CH_3), 1.61 (m, ^3J(H,H) = 4.6 Hz, 3H; CH_3), 1.95 (m, 2H; CH_2), 5.39 ppm (m, 2H; CH); ^{1}H NMR ([D$_6$]benzene, 25 °C): δ = 0.92 (t, ^3J(H,H) = 7.3 Hz, 3H; CH_3), 1.51 (m, ^3J(H,H) = 5.0 Hz, 3H; CH_3), 1.96 (m, 2H; CH_2), 5.42 ppm (m, 2H; CH); *trans*-2-pentene: ^{1}H NMR ([D$_8$]THF, 25 °C): δ = 0.94 (t, ^3J(H,H) = 7.3 Hz, 3H; CH_3), 1.58 (m, ^3J(H,H) = 5.0 Hz, 3H; CH_3), 1.95 (m, 2H; CH_2), 5.39 ppm (m, 2H; CH); ^{1}H NMR ([D$_6$]benzene, 25 °C): δ = 0.92 (t, ^3J(H,H) = 7.3 Hz, 3H; CH_3), 1.58 (m, ^3J(H,H) = 6.0 Hz, 3H; CH_3), 1.96 (m, 2H; CH_2), 5.42 ppm (m, 2H; CH).

2-Butene: MS: *m*/*z* (%): 56 (100) [M^+]; *cis*-2-butene: ^{1}H NMR ([D$_6$]benzene, 25 °C): δ = 1.50 (d, ^3J(H,H) = 4.9 Hz, 6H; CH_3), 5.47 ppm (m, 2H; CH); *trans*-2-butene: ^{1}H NMR ([D$_6$]benzene, 25°): δ = 1.57 (d, ^3J(H,H) = 4.9 Hz, 6H; CH_3), 5.47 ppm (m, 2H; CH).

3-Hexene: MS: *m*/*z* (%): 84 (50) [M^+], 69 (30) [M^+-CH_3], 55 (100) [M^+-2CH_3]; *cis*-3-hexene: ^{1}H NMR ([D$_6$]benzene, 25 °C): δ = 0.92 (t, ^3J-(H,H) = 7.3 Hz, 6H; CH_3), 1.57 (d, ^3J(H,H) = 4.5 Hz, 4H; CH_2), 5.39 ppm (m, 2H; CH); *trans*-3-hexene: ^{1}H NMR ([D$_6$]benzene, 25 °C): δ = 0.92 (t, ^3J(H,H) = 7.3 Hz, 6H; CH_3), 1.52 (d, ^3J(H,H) = 5.5 Hz, 4H; CH_2), 5.39 ppm (m, 2H; CH).

Typical procedure for the hydrosilylation of furfural: [D$_8$]THF or [D$_6$]benzene (0.6 mL) was added to complex **1-La**, **Y**, or **3-Y** (0.01 mmol) in a J. Young NMR tube. After dissolution of all solid, phenylsilane (54 mg, 0.50 mmol) and furfural (38 mg, 0.40 mmol) were added. The reaction was followed by ^{1}H NMR spectroscopy and GC-MS analysis.

Bis(furan-2-ylmethoxy)(phenyl)silane: ^{1}H NMR ([D$_6$]benzene, 25 °C): δ = 4.67 (s, 4H; CH_2), 5.25 (s, 1H; SiH), 6.02 (m, 2H; C4-H), 6.08 (m, 2H; C3-H), 7.06 (m, 2H; C5-H), 7.17 (m, 2H; *m*-Ph + *p*-Ph), 7.71 ppm (m, 1H; *o*-Ph).

Tris(furan-2-ylmethoxy)(phenyl)silane: ^{1}H NMR ([D$_6$]benzene, 25 °C): δ = 4.76 (s, 6H; CH_2), 6.02 (m, 3H; C4-H), 6.05 (m, 3H; C3-H), 7.06 (m, 3H; C5-H), 7.17 (m, 2H; *m*-Ph + *p*-Ph), 7.77 ppm (m, 1H; *o*-Ph).

Typical procedure for the hydrogenation of furfural in a reactor: In the glovebox, toluene (4 mL) was added to complex **4-Y** (5 mg, 0.01 mmol), **1-La** (5 mg, 0.01 mmol), or **3-Y** (9 mg, 0.01 mmol) in a miniclave with PTFE cover (Büchi). After dissolution of all solid, furfural (38 mg, 0.40 mmol) was added, and the reactor was closed and pressurized with hydrogen (p(H$_2$) = 5.5–7.0 bar). After 1–3 days of stirring at ambient tem-

perature, the pressure was released and the reactor was opened in a fume hood. For ^{1}H NMR analysis, a 0.1 mL sample of the reaction solution was taken and 0.5 mL [D_8]THF added. The neat reaction mixture was analyzed by GC-MS.

*2-Furfuryl alcohol (**C**)*: MS: *m*/*z* (%): 98 (100) [M^+], 97 (33) [M^+-1], 81 (49) [M^+-OH^-], 70 (49) [M^+-CO], 69 (49) [M^+-CO], 53 (53).

*Furfuryl 2-furoate (**D**)*: MS: *m*/*z* (%): 192 (1) [M^+], 97 (13) [$M^+-C_5H_3O_2$], 95 (32) [$M^+-C_5H_5O_2$], 81 (100) [$M^+-C_5H_3O_3$].

Typical procedure for the hydrogenation of furfural in a pressure NMR tube: A Teflon-screw-top pressure NMR tube (Wilmad) was filled with a stock solution of **4-Y** in [D_8]THF (0.15 mL, 0.3 mL; $c=0.05$ mmol mL^{-1}), a stock solution of furfural in [D_8]THF (0.15 mL, 0.3 mL; $c=2.0$ mmol mL^{-1}), and [D_8]THF (0.3 mL, 0 mL). The NMR tube was cooled with liquid nitrogen, connected to a Schlenk line, and evacuated. The NMR tube was then warmed to room temperature and after the solution had melted, pressurized with hydrogen ($p(H_2)=5$ bar) and placed into an oil bath at 50 °C. The conversion was followed by ^{1}H NMR spectroscopy and determined by GC-MS analysis after six days.

Typical procedure for hydride transfer: [D_8]THF (0.6 mL) was added to complex **3-Y** (1:2, 66 mg, 0.072 mmol; 1:4, 33 mg, 0.036 mmol; 1:8, 17 mg, 0.019 mmol; 1:13, 10 mg, 0.011 mmol) in a J. Young NMR tube. After dissolution of all solid, furfural (42 mg, 0.437 mmol) was added and the color of the solution turned from yellow to brown. The conversion was then followed by ^{1}H NMR spectroscopy and determined by GC-MS.

Acknowledgements

We gratefully acknowledge financial support from the Cluster of Excellence RWTH Aachen "Tailor-Made Fuels from Biomass". Dr. K. Beckerle is gratefully thanked for measurements as well as Dr. Y. Wan and Prof. Dr. U. Englert for recording the X-ray data.

[1] Biofuel reviews: a) G. W. Huber, S. A. Iborra, A. Corma, *Chem. Rev.* **2006**, *106*, 4044–4098; b) A. Loppinet-Serani, C. Aymonier, F. Cansell, *ChemSusChem* **2008**, *1*, 486–503; c) O. R. Inderwildi, D. A. King, *Energy Environ. Sci.* **2009**, *2*, 343–346; d) S. N. Naik, V. V. Goud, P. K. Rout, A. K. Dalai, *Renewable Sustainable Energy Rev.* **2010**, *14*, 578–597; e) X. Yan, O. R. Inderwildi, D. A. King, *Energy Environ. Sci.* **2010**, *3*, 190–197.

[2] Furfural review: A. S. Mamman, J.-M. Lee, Y.-C. Kim, I. T. Hwang, N.-J. Park, Y. K. Hwang, J.-S. Chang, J.-S. Hwang, *Biofuel. Bioprod. Bioref.* **2008**, *2*, 438–454.

[3] HMF: a) N. Yan, C. Zhao, C. Luo, P. J. Dyson, H. Liu, Y. Kou, *J. Am. Chem. Soc.* **2006**, *128*, 8714–8715; b) C. Li, Z. Zhang, Z. K. Zhao, *Tetrahedron Lett.* **2009**, *50*, 5403–5405; c) S. Hu, Z. Zhang, J. Song, Y. Zhou, B. Han, *Green Chem.* **2009**, *11*, 1746–1749.

[4] a) J. N. Chheda, G. W. Huber, J. A. Dumesic, *Angew. Chem.* **2007**, *119*, 7298–7318; *Angew. Chem. Int. Ed.* **2007**, *46*, 7164–7183; b) A. Corma, O. de la Torre, M. Renz, N. Villandier, *Angew. Chem.* **2011**, *123*, 2423–2426; *Angew. Chem. Int. Ed.* **2011**, *50*, 2375–2378.

[5] Cyclen and cyclen derivatives: a) H. Stetter, K. H. Mayer, *Chem. Ber.* **1961**, *94*, 1410–1416; b) M. Suchý, R. Hudson, *Eur. J. Org. Chem.* **2008**, 4847–4865; c) M. Ciampolini, M. Micheloni, N. Nardi, P. Paoletti, *J. Chem. Soc. Dalton Trans.* **1984**, 1357–1362.

[6] Other syntheses of **L**H: a) J. F. Pilichowski, J. M. Lehn, J. P. Sauvage, J. C. Gramain, *Tetrahedron* **1985**, *41*, 1959–1964; b) J. Huang, Z. Zhou, T. H. Chan, *Synthesis* **2009**, *14*, 2341–2344; c) A. D. Averin, A. V. Shukhaev, A. K. Buryak, F. Denat, R. Guilard, I. P. Beletskaya, *Macroheterocycles* **2009**, *2*, 281–285.

[7] a) M. Ohashi, M. Konkol, I. Del Rosal, R. Poteau, L. Maron, J. Okuda, *J. Am. Chem. Soc.* **2008**, *130*, 6920–6921; b) J. C. Buffet, J. Okuda, *Dalton Trans.* **2011**, *40*, 7748–7754.

[8] S. Standfuss, T. P. Spaniol, J. Okuda, *Eur. J. Inorg. Chem.* **2010**, 2987–2991.

[9] P. A. Cox in *The Elements: Their Origin, Abundance, and Distribution*, Oxford University Press, Oxford, UK, **1989**.

[10] E. Abinet, T. P. Spaniol, J. Okuda, *Chem. Asian J.* **2011**, *6*, 389–391.

[11] V. Boldrini, G. B. Giovenzana, R. Pagliarin, G. Palmisano, M. Sisti, *Tetrahedron Lett.* **2000**, *41*, 6527–6530.

[12] A. J. Blake, J. P. Danks, W.-S. Li, V. Lippolis, M. Schröder, *J. Chem. Soc. Dalton Trans.* **2000**, 3034–3040.

[13] $r(H)=r-r(D)$; r was calculated from the mean distance between the four nitrogen atoms and the centroid built by N1, N2, N3, and N4. $r(D)$ is the radius of the donor atoms. $r(N(sp^3))$ is used as a simplification for all cavity calculations because N1 (amido nitrogen) is an sp^2–sp^3 borderline case and $r(N(sp^3))=0.72$ Å and $r(N(sp^2))=0.66$ Å do not differ much; a) L. A. Drummond, K. Henrick, M. J. L. Kanagasundaram, L. F. Lindoy, M. McPartlin, P. A. Tasker, *Inorg. Chem.* **1982**, *21*, 3923–3927; b) V. J. Thom, C. C. Fox, J. C. A. Boeyens, R. D. Hancock, *J. Am. Chem. Soc.* **1984**, *106*, 5947–5955; c) R. D. Hancock, *Pure Appl. Chem.* **1986**, *58*, 1445–1452; d) E. C. Constable, in *Coordination Chemistry of Macrocyclic Compounds*, Oxford Chemistry Primers 72 (Ed.: J. Evans), Oxford University Press, New York, **1999**, pp. 20–21; e) J. Yoo, D. E. Reichert, M. J. Welch, *Chem. Commun.* **2003**, 766–767.

[14] a) C. Li, W. T. Wong, *Tetrahedron* **2004**, *60*, 5595–5601; b) B. Jagadish, G. L. Brickert-Albrecht, G. S. Nichol, E. A. Mash, N. Raghunand, *Tetrahedron Lett.* **2011**, *52*, 2058–2061.

[15] a) R. Taube, H. Windisch, S. Maiwald, H. Hemling, H. Schumann, *J. Organomet. Chem.* **1996**, *513*, 49–61; b) R. Taube, H. Windisch, H. Weißenborn, H. Hemling, H. Schumann, *J. Organomet. Chem.* **1997**, *548*, 229–236; c) L. F. Sánchez-Barba, D. L. Hughes, S. M. Humphrey, M. Bochmann, *Organometallics* **2005**, *24*, 3792–3799; d) D. Robert, E. Abinet, T. P. Spaniol, J. Okuda, *Chem. Eur. J.* **2009**, *15*, 11937–11947.

[16] a) T. K. Panda, A. G. Trambitas, T. Bannenberg, C. G. Hrib, S. Randoll, P. G. Jones, M. Tamm, *Inorg. Chem.* **2009**, *48*, 5462–5472; b) K. Krogh-Jespersen, M. D. Romanelli, J. H. Melman, T. J. Emge, J. G. Brennan, *Inorg. Chem.* **2010**, *49*, 552–560.

[17] G. Meier, T. Braun, *Angew. Chem.* **2009**, *121*, 1575–1577; *Angew. Chem. Int. Ed. Engl.* **2009**, *48*, 1546–1548.

[18] Structurally characterized Cp-supported lanthanum hydrides: a) Y. K. Gun′ko, P. B. Hitchcock, M. F. Lappert, *Organometallics* **2000**, *19*, 2832–2834; b) W. J. Evans, J. M. Perotti, J. W. Ziller, *J. Am. Chem. Soc.* **2005**, *127*, 3894–3909; c) W. J. Evans, J. M. Perotti, J. W. Ziller, *Inorg. Chem.* **2005**, *44*, 5820–5825; d) M. Nishiura, J. Baldamus, T. Shima, K. Mori, Z. Hou, *Chem. Eur. J.* **2011**, *17*, 5033–5044.

[19] a) J. Cheng, K. Saliu, G. Y. Kiel, M. J. Ferguson, R. McDonald, J. Takats, *Angew. Chem.* **2008**, *120*, 4988–4991; *Angew. Chem. Int. Ed.* **2008**, *47*, 4910–4913; b) J. Cheng, K. Saliu, M. J. Ferguson, R. McDonald, J. Takats, *J. Organomet. Chem.* **2010**, *695*, 2696–2702.

[20] a) Y. Luo, Z. Hou, *J. Phys. Chem. C.* **2008**, *112*, 635–638; b) M. Nishiura, Z. Hou, *Nat. Chem.* **2010**, *2*, 257–268.

[21] O. Minge, N. W. Mitzel, H. Schmidbaur, *Organometallics* **2002**, *21*, 680–684.

[22] a) E. Frainnet, V. Martel-Siegfried, E. Brousse, J. Dedier, *J. Organomet. Chem.* **1975**, *85*, 297–310; b) E. Frainnet, R. Bourhis, F. Simonin, F. Moulines, *J. Organomet. Chem.* **1976**, *105*, 17–31; c) S. Chakraborty, J. A. Krause, H. Guan, *Organometallics* **2009**, *28*, 582–586.

[23] Hydrosilylation of furfural: a) I. G. Iovel, Y. Goldberg, M. V. Shimanskaya, E. Lukevits, *Chemistry of Heterocyclic Compounds* **1987**, *23*, 23–27; b) Y. Goldberg, E. Abele, M. V. Shymanska, E. Lukevics, *J. Organomet. Chem.* **1991**, *410*, 127–133; c) T. Shibata, T. Toru, S. Mizuta, S. Nakamura, S. Ogawa, H. Fujimoto, *Jpn. Kokai Tokkyo Koho* **2007**, JP 2007291044 A; e) B. Marciniec in *Hydrosilylation: Advances in Silicon Science Vol. 1*, Springer, **2009**; d) M. Zhang, A. Zhang, *Appl. Organomet. Chem.* **2010**, *24*, 751–757.

[24] Hydrogenation with rare-earth metal complexes: a) G. Jeske, H. Lauke, H. Mauermann, P. N. Swepston, H. Schumann, T. J. Marks, *J. Am. Chem. Soc.* **1985**, *107*, 8091–8103; b) G. A. Molander, J. A. C. Romero, *Chem. Rev.* **2002**, *102*, 2161–2185.

[25] Deoxygenation: a) E. Furimsky, *Catal. Rev. Sci. Eng.* **1983**, *25*, 421–458; b) K. S. P. Rao, S. Khajamasthan, G. Muralidhar, K. V. R. Chary, V. S. Subrahmanyam, *J. Chem. Soc. Chem. Commun.* **1988**, 375–376; review: c) M. J. Girgis, B. C. Gates, *Ind. Eng. Chem. Res.* **1991**, *30*, 2021–2058; d) A. Centeno, R. Maggi, B. Delmon, *Stud. Surf. Sci. Catal.* **1999**, *127*, 77–84; e) E. Furimsky, *Appl. Catal. A* **2000**, *199*, 147–190; f) T.-R. Vijava, E. R. M. Saari, A. O. I. Krause, *Appl. Catal. A* **2001**, *209*, 33–43; g) J.-W. Choe, C.-S. Lee, *J. Ind. Eng. Chem.* **2004**, *10*, 239–246; h) A. Y. Bunch, X. Wang, U. S. Ozkan, *J. Mol. Catal. A* **2007**, *270*, 264–277; i) A. Y. Bunch, X. Wang, U. S. Ozkan, *Appl. Catal. A* **2008**, *346*, 96–103.

[26] C–O activation mediated by rare-earth metal complexes: a) S. N. Ringelberg, A. Meetsma, S. I. Troyanov, B. Hessen, J. H. Teuben, *Organometallics* **2002**, *21*, 1759–1765; b) S. Arndt, T. P. Spaniol, J. Okuda, *Organometallics* **2003**, *22*, 775–781; c) D. Cui, O. Tardif, Z. Hou, *J. Am. Chem. Soc.* **2004**, *126*, 1312–1313; d) T. Shima, Z. Hou, *J. Am. Chem. Soc.* **2006**, *128*, 8124–8125; e) J. Hitzbleck, J. Okuda, *Organometallics* **2007**, *26*, 3227–3235; f) Z. Hou, M. Nishiura, T. Shima, *Eur. J. Inorg. Chem.* **2007**, 2535–2545; g) L. Luconi, D. M. Lyubov, C. Bianchini, A. Rossin, C. Faggi, G. K. Fukin, A. V. Cherkasov, A. S. Shavyrin, A. A. Trifonov, G. Giambastiani, *Eur. J. Inorg. Chem.* **2010**, 608–620.

[27] Quantification of the alkanes was difficult because the signals of *n*-pentane overlap with those of propane, generated by the hydrogenation of the allyl ligands.

[28] F. Mongin, A. Bucher, J. P. Bazareau, O. Bayh, H. Awad, F. Trécourt, *Tetrahedron Lett.* **2005**, *46*, 7989–7992.

[29] a) Bruker, SAINT-Plus, Bruker AXS Inc., Madison, Wisconsin, USA, **1999**; b) Bruker, SADABS, Bruker AXS Inc., Madison, Wisconsion, USA, **2004**; c) A. L. Spek, *Acta Crystallogr. D* **2008**, *65*, 148–155; d) A. Altomare, G. Cascarano, C. Giacovazzo, A. Guagliardi, M. C. Burla, G. Polidori, M. Camalli, *J. Appl. Crystallogr.* **1993**, *26*, 343–350; e) G. M. Sheldrick, *Acta Crystallogr. A* **2008**, *64*, 112–122; f) L. Farrugia, *J. Appl. Crystallogr.* **1999**, *32*, 837–838; g) K. Brandenburg, *Diamond*, Crystal Impact GbR, Bonn, Germany, **2004**.

Received: July 12, 2011
Published online: December 1, 2011

